Accepted Manuscript

5,7-Disubstituted-[1,2,4]triazolo[1,5-a][1,3,5]triazines as Pharmacological Tools to Explore the Antagonist Selectivity Profiles Toward Adenosine Receptors

Stephanie Federico, Antonella Ciancetta, Nicola Porta, Sara Redenti, Giorgia Pastorin, Barbara Cacciari, Karl Norbert Klotz, Stefano Moro, Giampiero Spalluto

Please cite this article as: S. Federico, A. Ciancetta, N. Porta, S. Redenti, G. Pastorin, B. Cacciari, K.N. Klotz, S. Moro, G. Spalluto, 5,7-Disubstituted-[1,2,4]triazolo[1,5-a][1,3,5]triazines as Pharmacological Tools to Explore the Antagonist Selectivity Profiles Toward Adenosine Receptors, *European Journal of Medicinal Chemistry* (2016), doi: 10.1016/j.ejmech.2015.12.019.

K_i hA$_1$AR= 94.6 nM
K_i hA$_{2A}$AR= 1.11 nM
IC$_{50}$ hA$_{2B}$AR= 2,214 nM
K_i hA$_3$AR= 30.8 nM
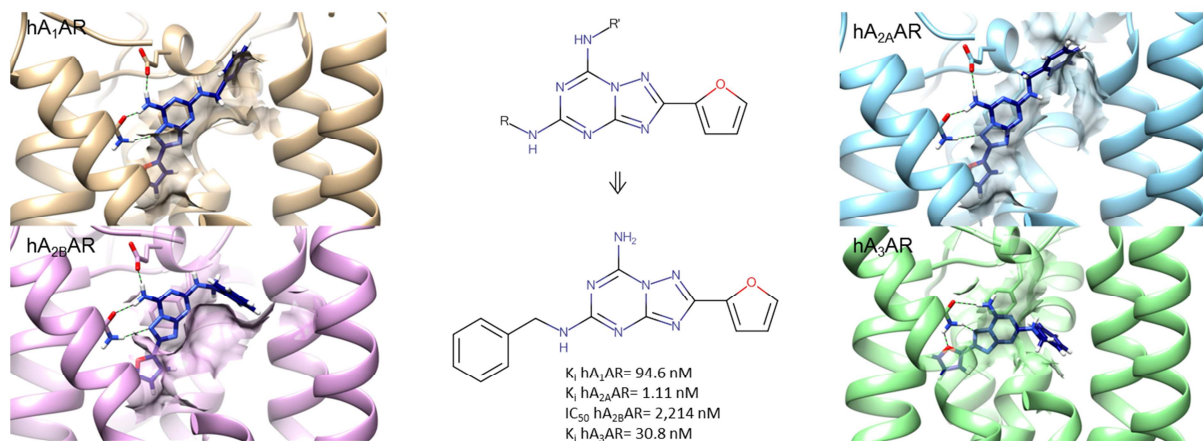
1 **5,7-Disubstituted-[1,2,4]triazolo[1,5-*a*][1,3,5]triazines as Pharmacological Tools to Explore the**

2 **Antagonist Selectivity Profiles Toward Adenosine Receptors.**

3

4 Stephanie Federico[a], Antonella Ciancetta[b], Nicola Porta[b], Sara Redenti[a], Giorgia Pastorin[c], Barbara

5 Cacciari[d], Karl Norbert Klotz[e], Stefano Moro[b]* and Giampiero Spalluto [a]*

6

7 [a]*Dipartimento di Scienze Chimiche e Farmaceutiche, Università di Trieste, Piazzale Europa 1,*

8 *34127 Trieste, Italy*

9 [b]*Molecular Modeling Section (MMS), Dipartimento di Scienze del Farmaco, Università di Padova,*

10 *via Marzolo 5, 35131 Padova, Italy*

11 [c]*Department of Pharmacy, National University of Singapore, 3 Science Drive 2, 117543 Singapore,*

12 *Singapore*

13 [d]*Dipartimento di Scienze Chimiche e Farmaceutiche, Università degli Studi di Ferrara, via Fossato*

14 *di Mortara 17-19, 44100 Ferrara, Italy*

15 [e]*Institut für Pharmakologie und Toxicologie, Universität of Würzburg, Versbacher Strasse 9, 97078*

16 *Würzburg, Germany*

17

18 *Corresponding authors*. Tel +39 040 5583726 (G.S.), +39 049 8275704 (S.M.); Fax +39 040

19 52572 (G.S.), +39 049 8275366 (S.M.); E-mail spalluto@units.it (G.S.), stefano.moro@unipd.it

20 (S.M.).

21
22
23
24
25
26
27
28
29
30
31

1 **Abstract**

2 The structure-activity relationship of new 5,7-disubstituted-[1,2,4]triazolo[1,5-*a*][1,3,5]triazines as

3 adenosine receptors (ARs) antagonists has been explored. The introduction of a benzylamino group

4 at C5 with a free amino group at C7 increases the affinity toward all the ARs subtypes (**10**: $K_i hA_1$ =

5 94.6 nM; $K_i hA_{2A}$ = 1.11 nM; $IC_{50} hA_{2B}$ = 2,214 nM; $K_i hA_3$ = 30.8 nM). Replacing the free amino

6 group at C7 with a phenylureido moiety yields a potent and quite selective hA_{2A} AR antagonist (**14**:

7 hA_{2A} AR K_i = 1.44 nM; hA_1/hA_{2A} = 216.0; hA_3/hA_{2A} = 20.6). This trend diverges from the analysis

8 on the pyrazolo[4,3-*e*][1,2,4]triazolo[1,5-*c*]pyrimidine series previously reported. With the help of

9 an in silico receptor-driven approach, we have rationalized these observations and elucidated from a

10 molecular point of view the role of the benzylamino group at C5 in determining affinity toward the

11 hA_{2A} AR.

12

15 **Abbreviations**. AR, adenosine receptor; CCPA, 2-chloro-N6-cyclopentyladenosine; CHO, Chinese

16 hamster ovary; IEele, per residue electrostatic contributions to the interaction energy; IEFs,

17 Interaction Energy Fingerprints; IEhyd, per residue hydrophobic contributions to the interaction

18 energy; NECA, 5'-N-ethylcarboxamidoadenosine; PTP, pyrazolo[4,3-*e*][1,2,4]triazolo[1,5-

19 *c*]pyrimidine; R-PIA, R-(-)-N6-(2-phenylpropyl)adenosine; TEA, triethylamine; ZM241385, 4-[2-

20 [7-amino-2-(2-furyl)-[1,2,4]triazolo[1,5-*a*][1,3,5]triazin-5-yl-amino]ethylphenol; TM,

21 transmembrane; TT, [1,2,4]triazolo[1,5-*a*][1,3,5]triazine; EL2, second extracellular loop.

22

1 **1. Introduction**

2

3 Adenosine receptors (ARs) are members of the G protein-coupled receptors (GPCRs) superfamily.

4 To date, four ARs subtypes - the A_1 AR, A_{2A} AR, A_{2B} AR, and A_3 AR - are currently known[1], that

5 exert their physiological functions through the activation or inhibition of various second messenger

6 systems. In particular, the modulation of adenylate cyclase activity is considered the principal

7 intracellular signal transduction mediated by these receptors[2,3]. Activation or blockade of ARs is

8 responsible for a wide range of effects in numerous organ systems suggesting potential therapeutic

9 applications of ARs modulators. In particular, the cardioprotective[4,5] and neuroprotective[6,7] effects

10 associated with ARs activation have been clearly demonstrated during periods of cardiac and

11 cerebral ischemia, respectively. Moreover, the use of antagonists of distinct AR subtypes could be

12 useful in the treatment of asthma[8,9] or neurological diseases such as Parkinson's disease[10].

13 In recent years, the synthesis of a large variety of ARs agonists and antagonists for the

14 pharmacological characterization of this GPCRs family has been reported[11]. Diverse classes of

15 heterocyclic derivatives have been proposed as ARs antagonists, exhibiting high levels of both

16 affinity and selectivity. Within this framework, our research groups have extensively investigated

17 the pyrazolo[4,3-*e*][1,2,4]triazolo[1,5-*c*]pyrimidine (PTP) nucleus as basis for the design of ARs

18 antagonists[12-23]. Through the modulation of the substitution pattern at the C5 (C5^{PTP}) and N7 (N7^{PTP})

19 positions, potent and selective human (h) A_{2A} AR and A_3 AR antagonists (compounds $\mathbf{A}$[15] and $\mathbf{B}$[18],

20 Chart 1) were reported. Nevertheless, these derivatives, likewise to other tricyclic structures, suffer

21 from limited aqueous solubility and require complicated synthetic routes. To overcome these

22 limitations, we explored in recent years the synthesis of simplified bicyclic systems, such as

23 [1,2,4]triazolo[1,5-*c*]pyrimidines[24], and [1,2,4]triazolo[1,5-*a*][1,3,5]triazines (TT)[25,22]. The TT

24 nucleus, in particular, represents one of the most appealing bicyclic cores. In fact, one of the most

25 potent and selective A_{2A} AR antagonists yet reported − 4-[2-[7-amino-2-(2-furyl)-

26 [1,2,4]triazolo[1,5-*a*][1,3,5]triazin-5-yl-amino]ethylphenol (ZM241385, Chart 2) − is based on this

3

1 scaffold[26,27]. This compound also binds with good affinity to the hA_{2B} AR (28 nM), and its tritiated

2 form is used as radioligand for this receptor subtype[28].

Ki hA_1 AR = 101 nM
Ki hA_{2A} AR = **2.80** nM
Ki hA_{2B} AR = 90 nM
Ki hA_3 AR = 300 nM

A

Ki hA_1 AR = 594 nM
Ki hA_{2A} AR = 381 nM
Ki hA_{2B} AR = 222 nM
Ki hA_3 AR = **0.16** nM

B
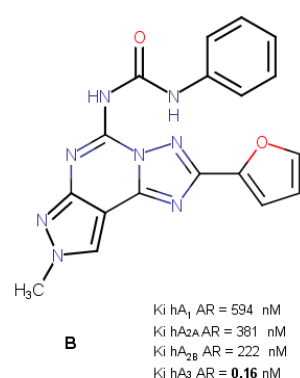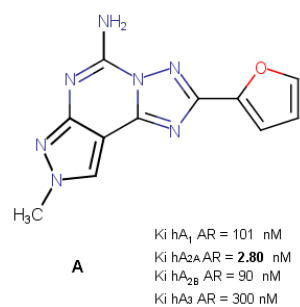
3

4 **Chart 1.** Previously reported pyrazolo[4,3-*e*][1,2,4]triazolo[1,5-*c*]pyrimidine as hARs antagonists.
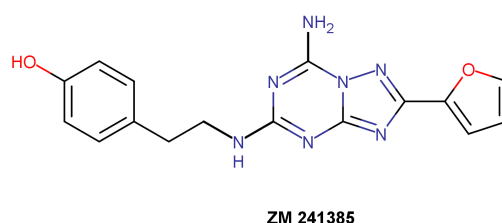
ZM 241385

5

6 **Chart 2.** Structure of ZM 241385.

7 In recent years[22], we explored the structure-activity-relationship (SAR) of the introduction at C5

8 position of the TT scaffold of solubilizing groups aimed at enhancing both the aqueous solubility

9 and the physicochemical properties. The resulting compounds maintained potency at the hA_{2A} AR

10 and, in some cases, subtype selectivity. In another study[25], we investigated the effect of the

11 substitutions at both the C5 and C7 position: compounds bearing a free amino group in C7 showed

12 good affinity at the rat (r) A_{2A} AR, whereas the introduction of a phenylureido moiety slightly

4

1   increased the affinity at the hA_3 AR with respect to the unsubstituted derivatives. In the present

2   study, we further explore both the C5 and C7 positions. The newly synthesized compounds have

3   been assessed at all four hARs, and the results rationalized from a molecular point of view with the

4   help of computational methodologies.

5   **2. Results and Discussion**

6   **2.1 Chemistry**

7   All the compounds were synthesized according to the procedure reported in Schemes 1-3. 5,7-

8   Diphenoxy-2-furoyl-[1,2,4]triazolo[1,5-*a*][1,3,5]triazine (**5**) and   7-amino-5-phenoxy-2-furoyl-

9   [1,2,4]triazolo[1,5-*a*][1,3,5]triazine (**6**) were obtained following the procedure reported in literature

10   by Caulkett et al. as depicted in Scheme 1[29].
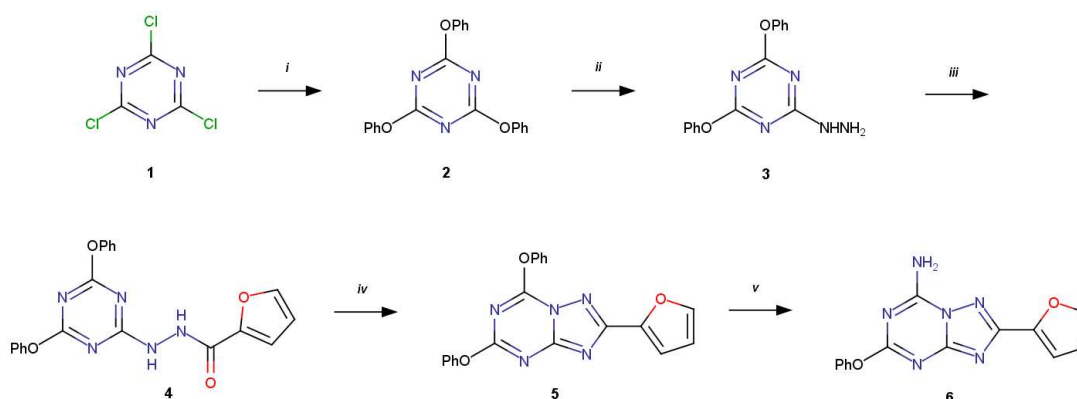
11

12   **Scheme 1. Reagents:** (i) PhOH, rfx, 5h; (ii) a. $NH_2NH_2.H_2O$, DCM, rt, 12h; b. *i*PrOH, rt, 14h; (iii)

13   2-furoylchloride, TEA, DCM, rt, 15h; (iv) P_2O_5, xylene, rfx, 14h; (v) NH_3/MeOH, rfx, 4h.

14   By reacting compound **6** with the appropriate amines in ethanol, in a sealed tube at 100 °C, the 7-

15   amino-5-aminosubstituted-2-furoyl-[1,2,4]triazolo[1,5-*a*][1,3,5]triazine   derivatives   (**7-10**)   were

16   obtained. Compounds **8-10** were already reported by Caulkett & coll[30]. Reaction of derivatives **7-10**

17   with phenylisocyanate gives the corresponding 7-phenylureas (**11-14**) while reaction with benzoyl

18   chloride or phenylacetyl chloride affords the corresponding 7-amido derivatives (**15-22**, Scheme 2).

5
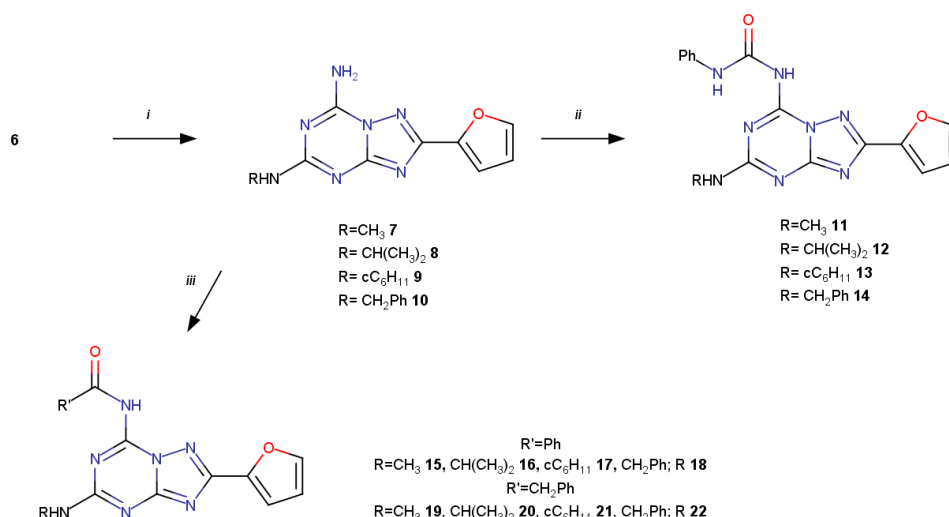
1

2 **Scheme 2. Reagents:** (i) NH$_2$R, EtOH, 100 °C, 3-72h; (ii) PhNCO, dioxane, rfx, 24h; (iii) R'COCl,

3 TEA, dioxane, rfx, 24h.

4 The synthetic pathway to obtain the 5,7-diaminosubstituted compounds (**26-37**) is reported in

5 Scheme 3. Firstly, the 5,7-diphenoxy-2-furoyl-[1,2,4]triazolo[1,5-*a*][1,3,5]triazine (**5**) was

6 substituted at the C5 position with different amines in ethanol, in a sealed tube at 60°C (**23-25**).

7 Then, the treatment of the obtained derivatives (**23-25**) with a second appropriate amine in ethanol,

8 in a sealed tube at 70-100 °C, yielded the desired 5,7-diaminosubstituted TT derivatives (**26,27,29-**

9 **32,34-36**). Compounds substituted with the same amino group both at the C5 and C7 positions

10 (**28,33,37**) were obtained by reaction between compound **5** and the desired amine at higher

11 temperature (90-120°C) or using amine in larger excess (5 eq).
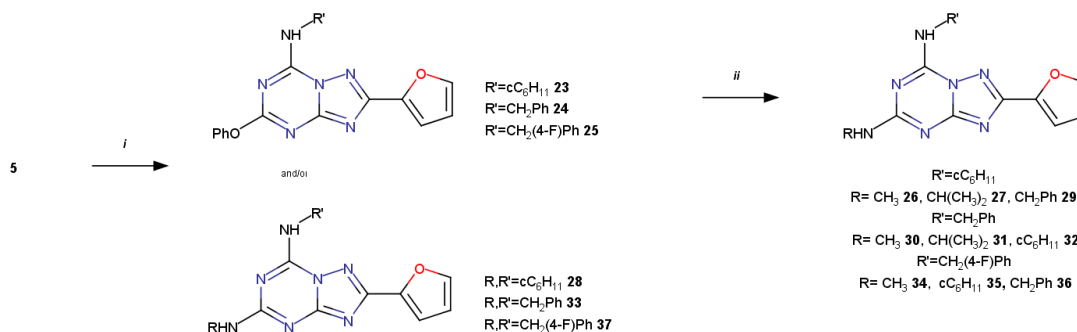
12

13 **Scheme 3. Reagents:** (i) NH$_2$R, EtOH, 60-120 °C, 3-24h; (ii) NH$_2$R', EtOH, 70-100 °C, 24-72h.

14

6

1 **2.2 Biological Activity**

2 The synthesized compounds (**7-37**) were tested at the human (h) A_1, A_{2A} and A_3 ARs expressed in

3 CHO cells: [^{3}H]CCPA (A_1), [^{3}H]NECA (A_{2A}) and [^{3}H]HEMADO (A_3) were used as radioligands in

4 binding assays[3], whereas the activity at the hA_{2B} AR was determined through the measurement of

5 the inhibition of NECA-stimulated adenylyl cyclase activity. The receptor binding affinities of the

6 synthesized compounds (**7-37**) are reported in Table 1. The derivatives can be divided into seven

7 subseries according to the substituent at the C7 position as compounds bearing: *(a)* a free amino (**7-**

8 **10**); *(b)* a phenylureido (**11-14**); *(c)* a benzamido (**15-18**); *(d)* a phenylacetamido (**19-22**); *(e)* a

9 cyclohexylamino (**23**, **26-29**); *(f)* a benzylamino (**24**, **30-33**); or *(g)* a 4-fluoro-benzylamino (**25**, **34-**

10 **37**) group.

11 All the derivatives display poor affinity toward the hA_1 AR. The most potent compounds toward

12 hA_1 AR (**9**, **10**, **29**) possess a K_i in the range 63.9-138 nM (i.e. **9**: $K_i hA_1$ = 138 nM; **10**: $K_i hA_1$ =

13 94.6 nM; 2**9**: $K_i hA_1$ = 63.9 nM) and belong to the free amino (**9**, **10**) or cyclohexylamino (**29**)

14 subseries. However, derivatives **9**, **10** and **29** show a better affinity at the hA_{2A} AR than at the hA_1

15 AR (**9**: $K_i hA_{2A}$ = 3.56 nM; **10**: $K_i hA_{2A}$ = 1.11 nM; 2**9**: $K_i hA_{2A}$ = 15.2 nM). In all the seven subseries,

16 a common trend can be observed regarding affinity at the hA_1 AR: the derivative bearing a

17 benzylamino moiety at the C5 position exhibits higher affinity with respect to the corresponding

18 alkylamino compounds (e.g. **18**: $K_i hA_1$ = 1,450 nM vs **15**: $K_i hA_1$ = 10,500 nM; **16**: $K_i hA_1$ = 24,400

19 nM and **17**: $K_i hA_1$ = 7,560 nM).

20 Concerning the hA_{2B} AR, the majority of the newly synthesized derivatives turned out to be inactive

21 with a IC_{50} value above 30 μM. The compounds showing IC_{50} values in the low micromolar range

22 bear the benzylamino moiety at the C5 position (**10**: $IC_{50} hA_{2B}$ = 2,214 nM; **14**: $IC_{50} hA_{2B}$ = 4,360

23 nM; **22**: $IC_{50} hA_{2B}$ = 7,617 nM; **33**: $IC_{50} hA_{2B}$ = 11,800 nM), except for compound **9**, which is

24 substituted with a cyclohexylamino group at the same position (**9**: $IC_{50} hA_{2B}$ = 1,450 nM).

25 At the hA_{2A} AR subtype, the most promising compounds belong to the free amino (**7-10**) and the

26 phenylureido (**11-14**) subseries. Interestingly, as also in part observed for the hA_1 AR, in all the

7

Table 1. Structures and binding profile of synthesized compounds **7-37**.

7-37
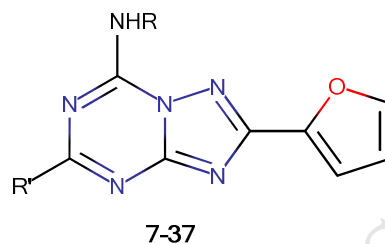
Compd	R	R'	hA$_1$ K$_i$ nM	hA$_{2A}$ K$_i$ nM	hA$_{2B}$ IC$_{50}$ nM	hA$_3$ K$_i$ nM	hA$_1$/hA$_{2A}$	hA$_3$/hA$_{2A}$
7	H	NHCH$_3$	2,570 (2,390 - 2,770)	49.3 (48.8 - 49.8)	> 30,000	1,560 (1,290 - 1,880)	52.1	31.6
8	H	NHCH(CH$_3$)$_2$	4,310 (4,220 - 4,410)	64.8 (53.3 - 78.7)	> 30,000	568 (481 - 671)	66.5	8.76
9	H	NHcC$_6$H$_{11}$	138 (133 - 143)	3.56 (2.53 - 5.02)	13,422 (8,500 – 21,193)	370 (330 - 415)	38.8	104
10	H	NHCH$_2$Ph	94.6 (89.6 - 99.9)	1.11 (0.83 - 1.48)	2,214 (1,209 – 4,053)	30.8 (26.8 - 35.5)	85.2	27.7
11	CONHPh	NHCH$_3$	3,850 (2,920 - 5,070)	99.6 (61.4 - 161)	> 30,000	572 (422 - 777)	38.6	5.74
12	CONHPh	NHCH(CH$_3$)$_2$	1,180 (1,090 - 1,270)	86.9 (54.7 - 138)	> 30,000	170 (145 - 199)	13.6	1.96
13	CONHPh	NHcC$_6$H$_{11}$	946 (475 - 1,890)	7.87 (4.90 - 12.7)	> 30,000	349 (335 - 364)	120	44.3

14	CONHPh	NHCH$_2$Ph	311 (171 - 568)	1.44 (1.29 - 1.60)	4,360 (1,991 – 9,548)	29.7 (24.3 - 36.2)	216	20.6
15	COPh	NHCH$_3$	10,500 (8,850 - 12,400)	194 (182 - 206)	> 30,000	9,240 (7,410 - 11,500)	54.1	47.6
16	COPh	NHCH(CH$_3$)$_2$	24,400 (20,800 - ~~~)	2,150 (2,040 - 2,270)	> 30,000	13,400 (11,900 - ~~~)	11.3	6.23
17	COPh	NHcC$_6$H$_{11}$	7,560 (6,390 - 8,940)	1,020 (828 - 1,250)	> 30,000	8,500 (8,170 - 8,840)	7.41	8.33
18	COPh	NHCH$_2$Ph	1,450 (1,170 - 1,800)	95.2 (75.3 - 120)	> 30,000	250 (241 - 258)	15.2	2.63
19	COCH$_2$Ph	NHCH$_3$	8,960 (8,460 - 9,500)	300 (212 - 424)	> 30,000	1,670 (1,400 - 1,980)	29.9	5.57
20	COCH$_2$Ph	NHCH(CH$_3$)$_2$	7,150 (6,640 - 7,700)	393 (289 - 533)	> 30,000	257 (228 - 290)	18.2	0.65
21	COCH$_2$Ph	NHcC$_6$H$_{11}$	1,010 (933 - 1,090)	23.6 (18.3 - 30.5)	> 30,000	286 (239 - 341)	42.8	12.1
22	COCH$_2$Ph	NHCH$_2$Ph	676 (619 - 737)	5.39 (4.32 - 6.73)	7,617 (4,080 - 14,223)	45.5 (38.6 - 53.7)	125	8.44
23	cC$_6$H$_{11}$	OPh	757 (575 - 997)	113 (85.8 - 148)	> 30,000	294 (262 - 329)	6.70	2.60
24	CH$_2$Ph	OPh	> 100,000	560 (457 - 686)	> 30,000	375 (362 - 389)	> 178	0.67
25	CH$_2$-4F-Ph	OPh	> 100,000	905 (632 - 1,300)	> 30,000	> 100,000	> 110	> 110
26	cC$_6$H$_{11}$	NHCH$_3$	361 (316 - 412)	143 (112 - 182)	> 30,000	905 (806 - 1,017)	2.52	6.33

27	cC$_6$H$_{11}$	NHCH(CH$_3$)$_2$	801 (723 - 888)	397 (313 - 502)	> 30,000	105 (90 - 121)	2.02	0.26
28	cC$_6$H$_{11}$	NHcC$_6$H$_{11}$	306 (299 - 313)	177 (122 - 256)	> 30,000	129 (112 - 147)	1.73	0.73
29	cC$_6$H$_{11}$	NHCH$_2$Ph	63.9 (59.1 - 69.1)	15.2 (13.7 - 16.9)	> 30,000	455 (351 - 590)	4.20	29.9
30	CH$_2$Ph	NHCH$_3$	2,770 (2,560 - 3,000)	173 (135 - 223)	> 30,000	275 (260 - 291)	16.0	1.59
31	CH$_2$Ph	NHCH(CH$_3$)$_2$	> 100,000	394 (242 - 643)	> 30,000	114 (108 - 121)	> 253	0.29
32	CH$_2$Ph	NHcC$_6$H$_{11}$	no data due to poor solubility					
33	CH$_2$Ph	NHCH$_2$Ph	784 (541 - 1,140)	20.4 (15.2 - 27.2)	11, 800 (6,373 - 21,932)	37.0 (34.2 - 40.0)	38.4	1.81
34	CH$_2$-4F-Ph	NHCH$_3$	3,080 (2,320 - 4,100)	235 (178 - 310)	> 30,000	557 (498 - 622)	13.1	2.37
35	CH$_2$-4F-Ph	NHcC$_6$H$_{11}$	> 100,000	112 (92.4 - 136)	> 30,000	1,300 (818 - 2,050)	> 893	11.6
36	CH$_2$-4F-Ph	NHCH$_2$Ph	1,490 (1,130 - 1,980)	21.8 (15.5 - 30.8)	> 30,000	75.3 (61.3 - 92.5)	68.3	3.45
37	CH$_2$-4F-Ph	NHCH$_2$-4F-Ph	> 100,000	43.6 (26.0 - 73.1)	> 30,000	123 (103 - 147)	> 2,293	2.82

reported subseries the benzylamino substituent at the C5 position gives the best results in terms of affinity at the hA_{2A} AR (i.e. **10**: K_ihA_{2A} = 1.11 nM; **14**: K_ihA_{2A} = 1.44; **18**: K_ihA_{2A} = 95.2 nM; **22**: K_ihA_{2A} = 5.39 nM; **29**: K_ihA_{2A} = 15.2; **33**: K_ihA_{2A} = 20.4; **36**: K_ihA_{2A} = 21.8). In particular, compound **10,** bearing a free amino group at the C7 position, is the most potent compound of the series with a K_i value of 1.11 nM at the hA_{2A} AR. Compared with the C7 free amino group, a benzamido moiety in position C7 leads to a detrimental effect (i.e. **18**: K_ihA_{2A} = 95.2 nM), a phenylacetamido moiety partially recovers the affinity (i.e. **22**: K_ihA_{2A} = 5.39 nM), whereas a phenylureido group restores the affinity (i.e. **14**: K_ihA_{2A} = 1.44 nM). Monoalkylamino substituents are also tolerated in position C7, as good affinity values are obtained with a cyclohexyl- (i.e. **29**: K_ihA_{2A} = 15.2 nM), benzyl- (i.e. **33**: K_ihA_{2A} = 20.4 nM) and 4-fluorobenzyl- (i.e. **36**: K_ihA_{2A} = 21.8 nM) amino groups, even though the free amino group ends up being the most promising substitution (i.e. **10**: K_ihA_{2A} = 1.11 nM). Compound **10** exhibits an 85- and 28-fold selectivity versus hA_1 and hA_3 ARs, respectively, whereas compound **14** (K_ihA_{2A} = 1.11 nM) shows a 216- and 20.6-fold selectivity against the same receptor subtypes. In the phenylureido subseries, the potency decreases in the following order benzyl- > cyclohexyl- > isopropyl- > methyl-amino group (i.e. **14**: K_ihA_{2A} = 1.44 nM > **13**: K_ihA_{2A} = 7.87 nM > **12**: K_ihA_{2A} = 86.9 nM > **11**: K_ihA_{2A} = 99.6 nM).

By analyzing the binding data at the hA_3 AR, it emerges that the newly synthetized derivatives do not show interesting affinity toward this AR subtype. As also observed for the other ARs, the best results in terms of affinity are obtained with a benzylamino group at C5 position (i.e. **10**: K_ihA_3 = 30.8 nM; **14**: K_ihA_3 = 29.7nM; **22**: K_ihA_3 = 45.5 nM; **33**: K_ihA_3 = 37.0 nM; **36**: K_ihA_3 = 75.3 nM). The best hA_3 AR antagonist obtained for the series is compound **14** (phenylureido series), which, further is also one of the most potent derivatives at the hA_{2A} AR (K_ihA_{2A} = 1.44 nM).

The introduction of an isopropylamino group at C5 position generally provides a more potent hA_3 AR antagonist than the cyclohexylamino group (e.g. **12**: K_ihA_3 = 170 nM vs **13**: K_ihA_3 = 349 nM). In fact, in the cyclohexylamino series, the C5-isopropylamino derivative (**27**) is the most potent hA_3

11

AR antagonist with a K_i of 105 nM with respect to the range of affinity (129-905 nM) of the other compounds (**26**, **28**, **29**). The introduction of a fluorine atom at the *para* position of the benzylamino group at C5 and/or C7 positions decreases the affinity at the hA_3 AR (e.g. **33**: K_ihA_3 = 37.0 nM vs **36**: K_ihA_3 = 75.3 nM vs **37**: K_ihA_3 = 123 nM)

In conclusion, biological data suggest that, with a few exceptions, the synthesized derivatives are potent hA_{2A} AR ligands. The affinity of the compounds toward this AR subtype is tuned by the substitution pattern at the C5 position, whereas the selectivity profile is modulated by the substituent linked to the C7 position. Interestingly, the introduction of a benzylamino group at C5 combined with a free amino group in C7 yields affinity toward all the ARs subtypes (**10**: K_ihA_1 = 94.6 nM; K_ihA_{2A} = 1.11 nM; $IC_{50}hA_{2B}$ = 2,214 nM; K_ihA_3 = 30.8 nM). The substitution of the free amino group at C7 with a phenylureido moiety narrows the affinity down to the hA_{2A} and hA_3 AR subtypes (**14**: K_ihA_{2A} = 1.44 nM; K_ihA_3 = 29.7 nM).

2.4 Molecular Modelling

To explain from a molecular point of view the observed binding data, we carried out docking simulations of the new derivatives by running a previously reported computational protocol[23]. Selected compounds were docked into the orthosteric pocket of the hA_{2A} AR X-ray structure (PDB code: 4EIY) and the putative TM binding site of a previously obtained hA_3 AR homology model[31]. The selection of the docking poses was based upon optimal interaction geometries with the residues surrounding the binding site and by focusing the attention on derivatives showing K_i values falling into the low nanomolar range (arbitrary cut-off = 100 nM). A general analysis of the thus selected binding modes was performed with the aim to identify the receptor residues involved in the binding. The analysis was derived by computing *per residue* electrostatic and hydrophobic contributions to the interaction energy (IEele and IEhyd, respectively) and by graphically transferring the data into "Interaction Energy Fingerprints" (IEFs) maps. A more detailed analysis for the ligands showing higher activity toward the hA_{2A} and hA_3 ARs subtypes was performed through the inspection of

12

individual docking poses, as reported in the following.

The IEele map for the hA$_{2A}$ AR subtype (Figure 1A) shows five regions of negative potential energy with the most intense corresponding to residues located in TM2, TM6 and EL2. The most effective polar interaction is established with Asn253 (6.55), whereas Tyr 271 (7.36), His250 (6.52) and to a lesser extent Tyr9 (1.35), Glu13 (1.39), Ser 277 (7.42), and Asn181 (5.42) are engaged in secondary interactions.
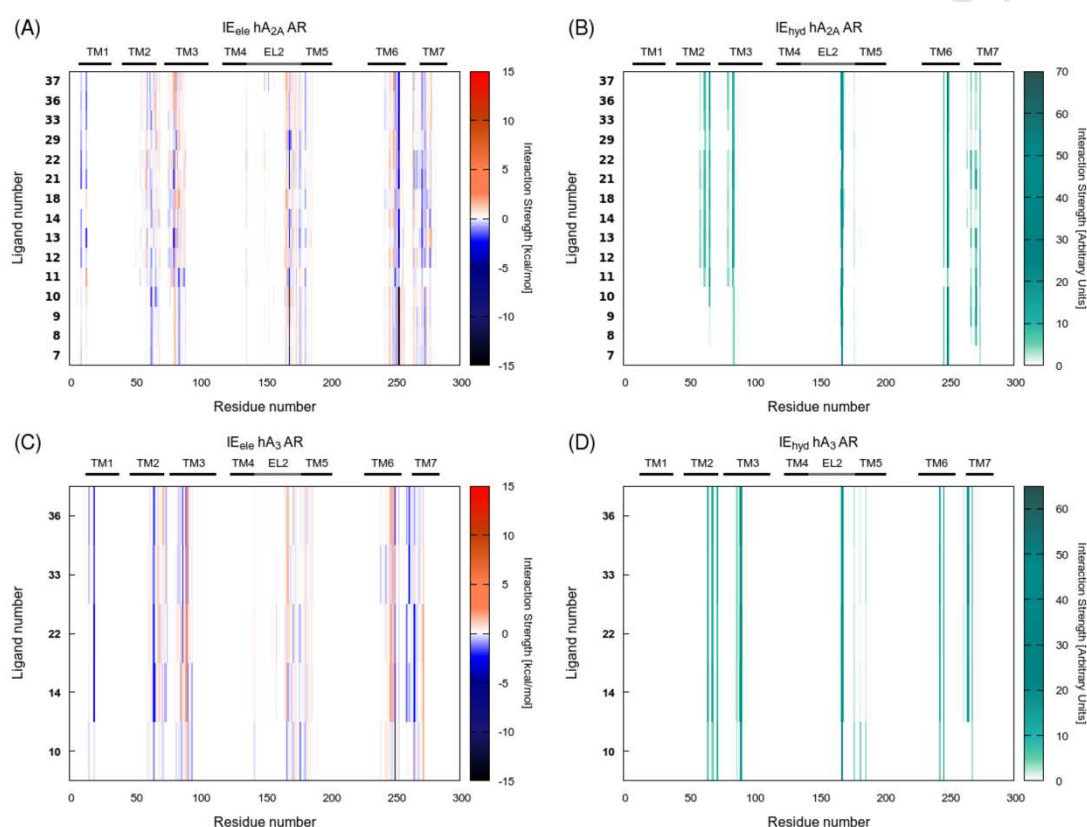
Figure 1. Per residue IEele and IEhyd maps for the most energetically favorable docking poses of compounds with Ki < 100 nM. The maps have been computed for selected poses of the considered compound inside the orthosteric binding site of hA$_{2A}$ AR (panels A and B) and the putative binding site of hA$_3$ AR (panels C and D). Electrostatic energy contributions are expressed in kcal/mol, whereas hydrophobic contributions are in arbitrary units. Ranges reported in the x-axes represent the length of protein sequences (truncated at 300 residues).

The IEhyd map (Figure 1B) displays several residues involved in hydrophobic contacts with the ligands, such as Phe168 (EL2) and Leu249 (6.51), Trp246 (6.48), Val84 (3.32), Ile274 (7.39), and Leu85 (3.33). Similar interaction patterns are also derived for the energetically more favourable poses of the ligands at the hA3 AR (Figure 1C and D): In particular, the most favourable electrostatic interactions involve Asn250 (6.55), while Tyr265 (7.36), Thr87 (3.29), and Glu19 (1.39) establish ancillary interactions. Hydrophobic contacts include, among others, Phe168 (EL2), Trp243 (6.48), Leu246 (6.51), Ile268 (7.39) and Leu90 (3.32).

A detailed analysis of the docking poses was performed for the most active compounds at the hA$_{2A}$ and the hA$_3$ ARs (derivatives **10** and **14**). As highlighted in the SAR analysis, the introduction of a benzylamino group at C5 and a free amino group in C7 yields affinity toward all the ARs subtypes (**10**: K$_i$hA$_1$ = 94.6 nM; K$_i$hA$_{2A}$ = 1.11 nM; IC$_{50}$hA$_{2B}$ = 2,214 nM; K$_i$hA$_3$ = 30.8 nM). In Figure 2 A-D the hypothetical binding modes of compound **10** at the four ARs subtypes is reported.
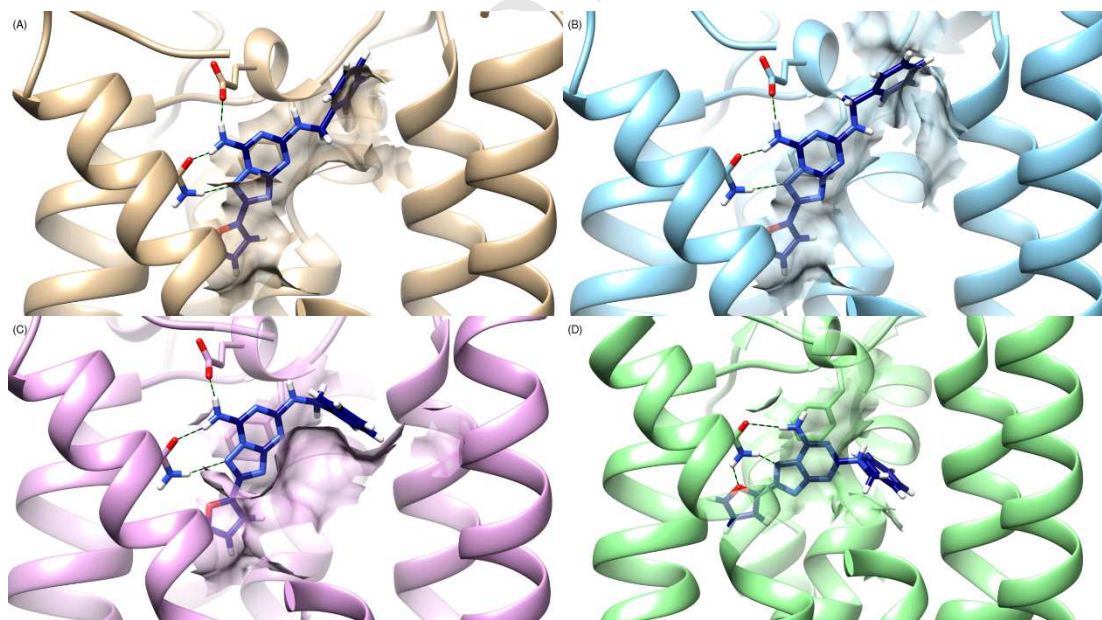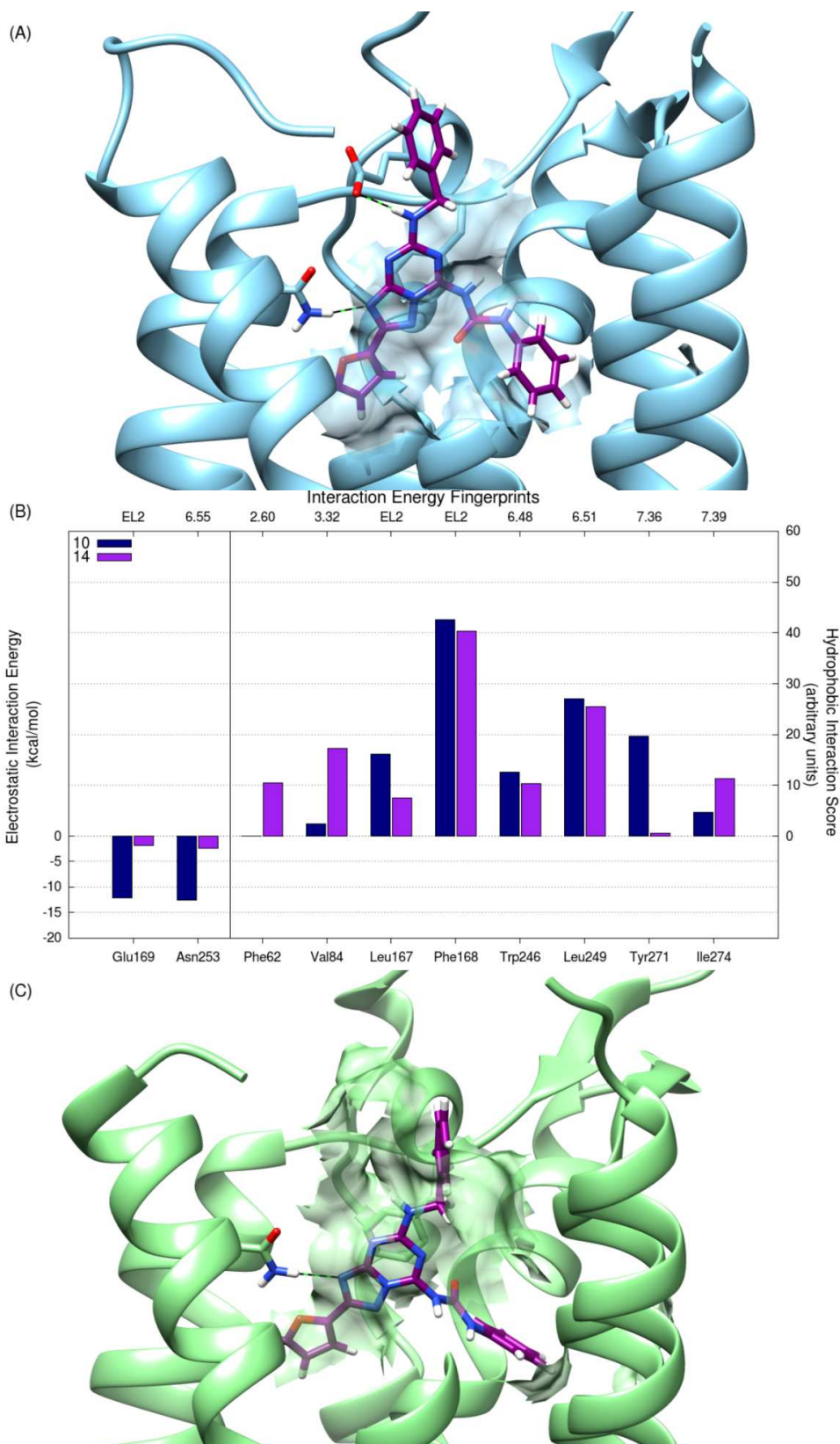

Figure 2. Hypothetical binding modes of compound **10** inside the hA$_1$ (A), hA$_{2A}$ (B), hA$_{2B}$ (C) and hA$_3$ (D) ARs binding sites. Poses are viewed from the membrane side facing TM6, TM7, and TM1, hydrogen bonds are highlighted as black dashed lines, and side chains of Asn (6.55), Phe (EL2), and

14

Glu (EL2) are represented as sticks. Residues interacting through hydrophobic contacts with the compounds are rendered as transparent surfaces.

As can be noted, in all the poses the ligand resides in the upper region of the transmembrane (TM) bundle, with the TT core anchored by an aromatic $\pi-\pi$ stacking interaction with Phe (EL2) and the furan ring pointing toward TM6 (see also Video S1). In particular, at the hA_1, hA_{2A}, and hA_{2B} ARs, (Figure 2 A, B, and C, respectively) the scaffold is anchored in the cleft by three hydrogen bonds established by the free amino group at the C7 position and the N2 of the triazole ring with the conserved Asn (6.55) and the Glu (EL2) residues. The ligand adopts a conformation that is superimposable with the crystallographic binding mode of ZM 241385 at the hA_{2A} AR (data not shown) with the substituent at C5 exposed toward the extracellular side and interacting with Tyr (7.36) at the hA_1 and hA_{2A} ARs (transparent surfaces in Figure 2A and 2C). The predicted binding mode at the hA_3 AR (Figure 2D) envisages the scaffold shifted toward TM2 with respect to the pose observed at the other ARs subtypes. We ascribe this different placement to the lack of the anchoring hydrogen bond played by Glu (EL2) at the other ARs subtypes, residue that is replaced by a valine in the hA_3 AR.

As mentioned in the SAR analysis, the introduction of a phenylureido group at C7 in place of a free amino group maintaining the benzylamino moiety at the C5 narrows the activity spectrum toward the hA_{2A} and hA_3 AR stubtypes (**14**: $K_ihA_{2A} = 1.44$ nM; $K_ihA_3 = 29.7$ nM). In the hypothetical binding mode of compound **14** at the hA_{2A} AR ($K_i = 1.44$ nM, Figure 3A), the scaffold is flipped by about 180 degrees with respect to the predicted placement of compound **10** (Figure 2B). The nitrogen of the benzylamino group at the C5 position establishes a hydrogen bond interaction with the Glu169 (EL2) sidechain, whereas the N4 of the triazole ring interacts with Asn253 (6.55). In this position the phenylureido group at C7 points between TM2 and TM3 and establishes hydrophobic contacts with Phe62 (2.60), Val84 (3.32), and Ile274 (7.39), represented as transparent surfaces in Figure 3A.

15

(A)

Interaction Energy Fingerprints

(B)

(C)

Figure 3. (A) Hypothetical binding mode of compound **14** inside the putative binding site of the

hA$_{2A}$ AR. The pose is viewed from the membrane side facing TM6, TM7, and TM1, hydrogen

bonds are highlighted as dashed black lines, and side chains of Asn253 (6.55), Phe168 (EL2), and

Glu169 (EL2) are represented as sticks. Residues interacting through hydrophobic contacts are rendered as transparent surfaces. (B) Interaction Energy Fingerprints (IEFs) for the most active compounds at the hA$_{2A}$ AR (**10**, **14**): Electrostatic energy contributions are expressed in kcal/mol, whereas hydrophobic contributions are in arbitrary units. (C) Hypothetical binding mode of compound **14** inside the putative binding site of hA$_3$ AR. The pose is viewed from the membrane side facing TM6, TM7, and TM1, hydrogen bonds are highlighted as dashed black lines, and side chains of Asn250 (6.55) and Phe168 (EL2) are represented as sticks. Residues interacting through hydrophobic contacts are rendered as transparent surfaces.

Consistently to the above described hypothetical binding modes, the IEFs analyses for compounds **10** and **14** at the hA$_{2A}$ AR (Figure 3B) identify Asn253 (6.55), Glu169 (EL2) and Phe168 (EL2) as the residues mainly contributing to the interaction energy, whereas different interaction patterns are observed for residues belonging to TM2, TM3, and TM7. These patterns, therefore, give rise to the different orientations of the TT scaffold, as depicted in Figure 2B and 3A. A similar trend - *e.g.* different binding modes depending on the nature of the substituents - was also previously observed for 5-alkylaminopyrazolo-[4,3-*e*][1,2,4]triazolo[1,5-*c*]pyrimidine[23] and 5,8-disubstituted-[1,2,4]triazolo[1,5-*c*]pyrymidine[24] derivatives.

The hypothetical binding mode of **14** at the hA$_3$ AR (Figure 3C) suggests that the compound might adopts a binding mode similar for the one observed at the hA$_{2A}$ AR. The main interactions are established with Glu19 (1.39), Asn250 (6.55) and Phe168 (EL2) and an extended pattern of hydrophobic interactions involves with residues located in TM2, TM3 and TM7. With respect to the pose in the hA$_{2A}$ AR, the scaffold is shifted toward TM2. Again, as also observed for compound **10**, this shift might arise from the lack of the anchoring hydrogen bond (played by Glu169 at the hA$_{2A}$ AR, replaced by a valine residue in the hA$_3$ AR).

In order to explain and capture from a molecular point of view the signatures of the activity of the TT scaffold at the hARs, we performed a retrospective analysis by comparing the effect of

17

the substitution at positions C5 and C7 on corresponding analogues belonging to the PTP series previously reported[15,18]. In this analysis, we focused our attention on: (*a*) the effect of the introduction of a phenylureido moiety in place of the free amino group at C7 (corresponding to C5^{PTP}) position; (*b*) the effect of the introduction of a benzylamino substituent at C5 position, corresponding to the opening of the pyrazole ring of the PTP scaffold (see Chart 3).
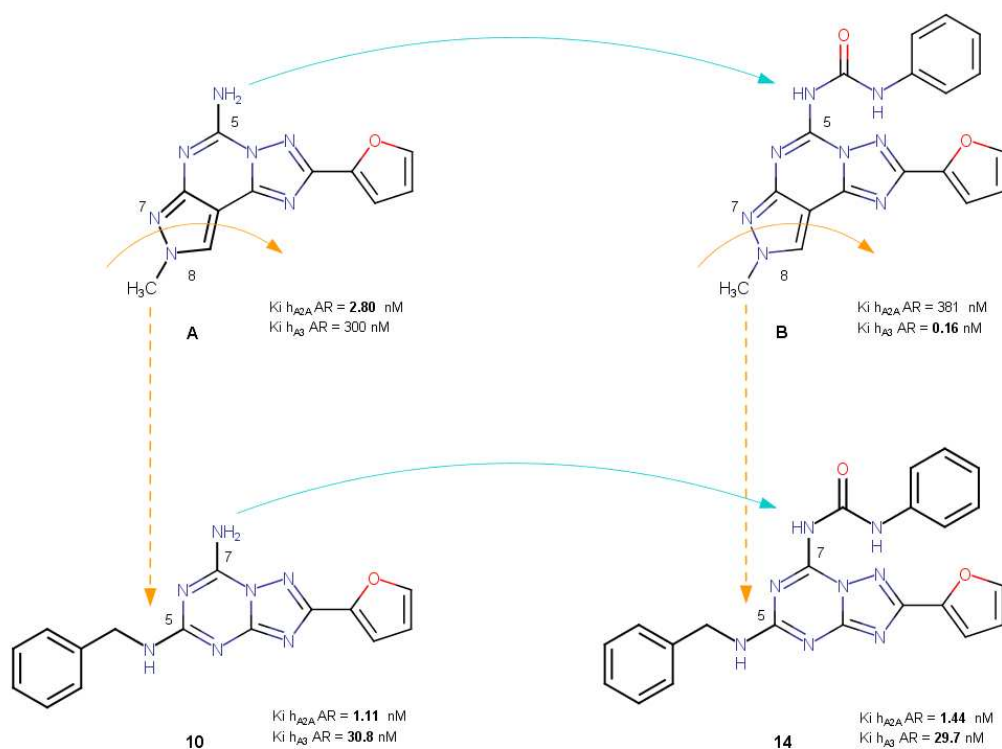
Chart 3. Structures of pyrazolo[4,3-*e*][1,2,4]triazolo[1,5-*c*]pyrimidines and [1,2,4]triazolo[1,5-*a*][1,3,5]triazines considered in the retrospective analysis.

As sketched out in Chart 3, the substitution of a free amino group in C5^{PTP} position with a phenylureido moiety causes a shift of the activity from the hA$_{2A}$ AR to the hA$_3$ AR. In the hypothetical binding modes of compound **A** at hA$_{2A}$ AR (Figure 4A) the free amino group at C5^{PTP} establishes a tight hydrogen bond network with Ans253 (6.55) and Glu169 (EL2), and the PTP scaffold is placed with the furan ring pointing toward TM6. In the hypothetical binding mode of compound **B** at the hA$_3$ AR (Figure 4B), the PTP scaffold is turned with the furan ring pointing toward TM3 and the phenylureido group exposed toward the extracellular side. The only anchoring

18

hydrogen bond in the binding site is established with Ans250 (6.55) through the N7 of the pyrazole ring. These data are consistent with previously reported modelling studies[23]: the presence of polar (charged) residues (Glu169, His264) in the binding site of the hA_{2A} AR does not allow ligands with bulky substituents (a phenylureido group in this case) to establish effective interactions. On the other side, these ligands are better accommodated at the hA_3 AR which binding site lacks charge residues (Glu169 is mutated to Val169).
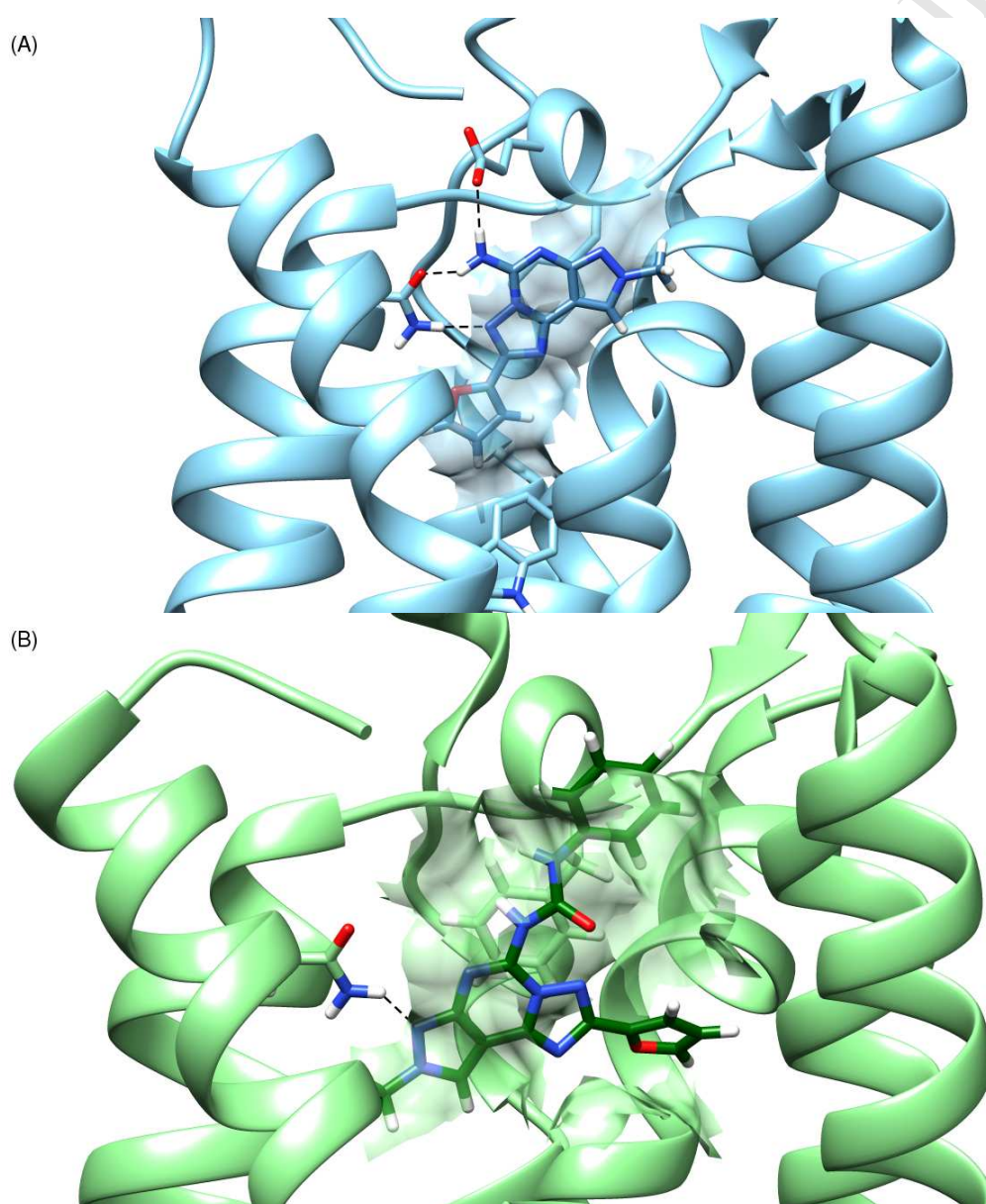
Figure 4. Hypothetical binding modes of previously reported compound **A** (A) and **B** (B) inside the orthosteric binding site of hA_{2A} AR and the putative binding cleft of hA_3 AR, respectively. Poses are viewed from the membrane side facing TM6, TM7, and TM1, hydrogen bonds are

19

highlighted as black dashed lines, and side chains of receptor main residues involved in the binding are represented as sticks. Residues interacting through hydrophobic contacts with the compounds are rendered as transparent surfaces.

The same substitution on the TT scaffold, however, does not produce the same shift of the activity (Chart 3). In fact, the introduction of a phenylureido group at C7 confers activity at both ARs subtypes. The retained affinity at the hA_{2A} AR, in particular, can be ascribed to the presence of the benzylamino group at C5: the nitrogen atom of this moiety (compound **14**, Figure 2C) establishes a hydrogen bond interaction with Glu169 (EL2) that counterbalances the disruption of the hydrogen bond network provided by the free amino group at C7 (compound **10**, Figure 2B). Within the PTP series this balance of interactions is not possible due to the geometric constraints imposed by the pyrazole ring.

3. Conclusions

We have presented a novel series of 5,7-disubstituted-[1,2,4]triazolo[1,5-*a*][1,3,5]triazines as adenosine receptors antagonists. The SAR analysis has revealed that the newly synthetized compounds show affinity for the hA_{2A} and hA_3 ARs depending on the substitution patterns at the C5 and C7 positions. In particular, the substituent at C5 tunes the potency of the compounds, whereas the moiety linked to C7 modulates the selectivity profile. A benzylamino group at the C5 position combined with a free amino group at the C7 position yields affinity toward all the ARs subtypes (compound **10**: $K_ihA_1 = 94.6$ nM; $K_ihA_{2A} = 1.11$ nM; $IC_{50}hA_{2B} = 2,214$ nM; $K_ihA_3 = 30.8$ nM). The replacement of the free amino group at C7 with a phenylureido moiety yields a potent and quite selective hA_{2A} AR antagonist (compound **14**: hA_{2A} AR $K_i = 1.44$ nM; $hA_1/hA_{2A} = 216.0$; $hA_3/hA_{2A} = 20.6$) and narrows the activity spectrum toward the hA_{2A} and the hA_3 AR subtypes. The observed trend diverges from the analyses on the pyrazolo-[4,3-*e*][1,2,4]triazolo[1,5-*c*]pyrimidine (PTP) series we have reported on in the past. With the help of an *in silico* receptor-driven approach,

we have elucidated that the key to retain activity at the hA$_{2A}$ AR resides in the substituent attached at C5: the benzylamino group interacts with the Glu169 (EL2) thus counterbalancing the loss of the hydrogen bond network provided by the free amino group at C7. On the other side, the static depiction on the final stage of the ligand recognition offered by the docking approach does not allow to fully explain the selectivity profile of the newly synthetized compounds thus suggesting that the selectivity game might be played prior the ligand reaches the orthosteric site. To this aim, a better depiction could be offered by methodologies that take into account the time-dependent evolution of the molecular system, such as classical or biased/supervised molecular dynamics approaches.

4. Experimental Section

4.1 Chemistry

General. Reactions were routinely monitored by thin-layer chromatography (TLC) on silica gel (precoated F$_{254}$ Macherey-Nagel aluminium sheets). Flash chromatography was performed using Macherey-Nagel 230-400 mesh silica gel or Macherey-Nagel aluminium oxide 90 neutral. Light petroleum ether refers to the fractions boiling at 40-60 °C. Melting points were determined on a Büchi-Tottoli instrument and are uncorrected. ^{1}H-NMR were determined in CDCl$_3$, DMSO-d$_6$, acetone-d$_6$ or CD$_3$OD solutions with a Varian Gemini 200 spectrometer (University of Trieste), peaks positions are given in parts per million (δ) downfield relative to the central peak of the solvents, and J values are given in Hz. The following abbreviations were used: s, singlet; bs, broad singlet; d, doublet; dd, double doublet; bd, broad doublet; t, triplet; m, multiplet. Electrospray mass spectra were recorded on an ESI Bruker 4000 Esquire spectrometer, and compounds were dissolved in methanol. Elemental analyses indicated by the symbols of the elements were performed by the microanalytical laboratory of Dipartimento di Scienze Chimiche e Farmaceutiche, University of Trieste, and were within ± 0.4% of the theoretical values for C, H, and N.

Synthesis of 2,4,6-triphenoxy-[1,3,5]triazine (2). A mixture of the commercial available cyanuric

21

chloride (184.4 g, 1.0 mol) was dissolved in phenol (3.0-4.0 mol) and refluxed for 5h. The hot reaction was extracted with methanol and a white solid was obtained. Yield quantitative; mp 235°C; ^{1}H-NMR (CDCl$_3$) δ: 7.29-7.42 (m, 6H), 7.17-7.25 (m, 3H), 7.07-7.17 (m, 6H).

Synthesis of (4,6-diphenoxy-[1,3,5]triazin-2-yl)-hydrazine (3). To a solution of compound **2** (36 g, 0.1 mol) in dichloromethane (500 mL), hydrazine monohydrate was added (5 mL, 0.1 mol) and the reaction was stirred overnight. The solvent was removed and the residue suspended in isopropanol (300 mL) and stirred for 14 hours. Then the white solid was filtered off and 24.5 g of title compound were obtained (24.5 g). Yield 83%; mp 107 °C; ^{1}H-NMR (DMSO-d$_6$) δ: 4.34 (bs, 2H), 7.12-7.30 (m, 6H), 7.35-7.46 (m, 4H), 9.20 (bs, 1H).

Synthesis of furan-2-carboxylic acid N'-(4,6-diphenoxy[1,3,5]triazin-2-yl)-hydrazide (4). Compound **3** (24.5 g, 0.083 mol) was dissolved in dichloromethane (240 mL), triethylamine (TEA) (11.6 mL, 0.083 mol) was added the solution, and then a solution of 2-furoyl chloride (4.91 mL, 0.05 mol) in dichloromethane (60 mL) was added slowly maintaining reaction at 0°C. The mixture was stirred for 3 hours then 2-furoyl chloride was added again (3.27 g, 0.033 mol) and the reaction was stirred for 12 hours at room temperature. The mixture was washed with water (2x200 mL) and brine (100 mL). The organic layer was dried, concentrated and purified by flash chromatography (EtOAc 4/ Light petroleum 6) to provide compound **4** as a white solid (16.1 g). Yield 49.8%; mp 183 °C; ^{1}H-NMR (CDCl$_3$) δ: 6.7 (dd, *J*=1.8, *J*=3.4, 1H), 7.12-7.45 (m, 13H), 8.28 (bs, 1H).

Synthesis of 2-furan-2-yl-5,7-diphenoxy-[1,2,4]triazolo[1,5-a][1,3,5]triazine (5). The hydrazide derivative **4** (7.0 g, 0.018 mol) was dissolved in xylene (250 mL) and P$_2$O$_5$ (17 g, 0.12 mol) was added and the mixture was refluxed for 14 hours. The solvent was removed under reduced pressure and the residue was dissolved in dichloromethane (250 mL) and washed with a mixture of water and brine (3 x 80 mL). The organic layer was dried, concentrated and purified by flash chromatography (EtOAc 2/ Light Petroleum 8) to provide compound **5** as a white solid (1.4 g). Yield 21%; mp 246-248 °C; ^{1}H-NMR (CDCl$_3$) δ: 6.59 (dd, *J*=1.8, *J*=3.2, 1H), 7.11-7.51 (m, 11H), 7.63 (s, 1H).

22

Synthesis of 2-furan-2-yl-5-phenoxy-[1,2,4]triazolo[1,5-a][1,3,5]triazin-7-ylamine (6). To a solution of compound **5** (580 mg, 1.56 mmol) in methanol (40 mL) 5 mL of ammonia 7N solution in methanol were added, the reaction was then refluxed for 4 hours. The solvent was removed under reduced pressure; the residue was purified by column chromatography (EtOAc 3/ Light petroleum 7) and precipitated from diethyl ether and light petroleum, providing the desired compound **6** as white solid (423 mg). Yield 92%; white solid; mp 253 °C (EtOAc-Light petroleum); ^{1}H-NMR (DMSO-d_6) δ: 6.70 (dd, J=2, J=3.2, 1H), 7.12 (d, J=3.2, 1H), 7.22-7.31 (m, 3H), 7.42-7.49 (m, 2H), 7.91 (d, J=2, 1H), 8.99 (bd, 2H).

General procedure for the synthesis of N^5-substituted-2-furan-2-yl-[1,2,4]triazolo[1,5-a][1,3,5]triazine-5,7-diamine (7-10). Compound **6** was dissolved in ethanol and 1.5-10 eq of the desired amine were added. Reaction was stirred in a sealed tube at 100°C for a time that could vary from 3 to 72 hours. Reaction was monitored by TLC using EtOAc 1/ Light petroleum 1 as eluent. The solvent was then removed and the residue was purified by column chromatography to give the desired compound. The solid was suspended in EtOAc, precipitated with light petroleum and filtered.

*2-(Furan-2-yl)-N^5-methyl-[1,2,4]triazolo[1,5-a][1,3,5]triazine-5,7-diamine (**7**)*. 1g (3.40 mmol) of compound **6** was reacted with 2.11 mL of methylamine 33 wt. % solution in ethanol (17 mmol, 5 eq) for 4 hours. Eluent of column chromatography was EtOAc. White solid (300 mg, 38%); mp 244 °C; ^{1}H-NMR (DMSO-d_6) δ: 2.79 (d, J=4.8, 3H); 6.68 (s, 1H); 7.04 (s, 1H); 7.32-7.42 (m, 1H); 7.86 (s, 1H); 8.14 (bs, 2H). IR (Nujol) cm^{-1}: 3284, 2884, 1657, 1586, 1514, 1496, 1407, 1369, 1316, 1227, 910, 773. Anal. ($C_9H_9N_7O$) C, H, N.

*2-Furan-2-yl-N^5-isopropyl-[1,2,4]triazolo[1,5-a][1,3,5]triazin-5,7-diamine (**8**)*. 485 mg (1.65 mmol) of compound **6** were reacted with 1.4 mL of isopropylamine (16.5 mmol, 10 eq) for 24 hours. Column chromatography with gradient elution starting at EtOAc 4/ Light petroleum 6 and ending at EtOAc 9/ Light petroleum 1. White solid (370 mg, 86.6%); mp 209 °C; ^{1}H-NMR (DMSO-d_6) δ: 1.14 (d, J=6.6, 6H); 4.01-4.10 (m, 1H); 6.63 (s, 1H); 7.04 (s, 1H); 7.29 (d, J=7.8, 1H); 7.86 (s, 1H);

8.07 (bs, 2H). IR (Nujol) cm^{-1}: 3418, 2876, 1659, 1608, 1572, 1514, 1362, 1324, 1182, 783, 699. Anal. ($C_{11}H_{13}N_7O$) C, H, N.

N^5-Cyclohexyl-2-furan-2-yl-[1,2,4]triazolo[1,5-a][1,3,5]triazin-5,7-diamine *(9)*. 500 mg (1.70 mmol) of compound **6** were reacted with 0.97 mL of cyclohexylamine (8.5 mmol, 5 eq) for 4 hours. Eluent of column chromatography was EtOAc 8/ Dichloromethane 2. White solid (195 mg, 38.3%); mp >250 °C; ^{1}H-NMR (DMSO-d$_6$) δ: 1.20-1.28 (m, 5H); 1.57-1.90 (m, 5H); 3.72 (bs, 1H); 6.67 (s, 1H); 7.04 (s, 1H); 7.32 (d, *J*=8.4, 1H); 7.86 (s, 1H); 8.07 (bs, 2H). IR (Nujol) cm^{-1}: 3440, 2919, 2853, 1667, 1624, 1590, 1493, 1408, 1322, 1011, 765, 738. Anal. ($C_{14}H_{17}N_7O$) C, H, N. In this reaction were obtained also 160 mg of N^5,N^7-dicyclohexyl-2-(furan-2-yl)-[1,2,4]triazolo[1,5-a][1,3,5]triazine-5,7-diamine (**28**, 24.7%).

N^5-Benzyl-2-furan-2-yl-[1,2,4]triazolo[1,5-a][1,3,5]triazin-5,7-diamine *(10)*. 500 mg (1.70 mmol) of compound **6** were reacted with 0.28 mL of benzylamine (2.55 mmol, 1.5 eq) for 72 hours. Eluent of column chromatography was EtOAc 8/ Dichloromethane 2. Pale yellow solid (140 mg, 26.8%); mp 157 °C; ^{1}H-NMR (DMSO-d$_6$) δ: 4.52 (s, 2H); 6.66 (s, 1H); 7.05 (s, 1H); 7.10-7.42 (m, 5H); 7.86 (s, 1H); 7.99 (bs, 1H); 8.23 (bs, 2H). IR (Nujol) cm^{-1}: 3418, 2072, 1655, 1650, 1632, 1588, 1504, 1486, 1415, 1322, 770, 621. Anal. ($C_{15}H_{13}N_7O$) C, H, N.

General procedure for the synthesis of 1-(2-(furan-2-yl)-5-(substitutedamino)-[1,2,4]triazolo[1,5-a][1,3,5]triazin-7-yl)-3-phenylurea (11-14). The appropriate N^5-substituted-2-furan-2-yl-[1,2,4]triazolo[1,5-a][1,3,5]triazine-5,7-diamine (**7-10**, 0.3 mmol) was dissolved in 5 mL of dry 1,4-dioxane and 0.45 mmol of phenylisocyanate (49 µL, 1.5 eq) were added. The solution was stirred at reflux for 24h. The reaction was monitored by TLC (EtOAc 3/ light petroleum 7 or EtOAc 4/ Light petroleum 6). The solvent was then removed and the residue was purified by column chromatography (EtOAc 3/ Light petroleum 7) to give the desired compound (**11-14**). The solid was suspended in EtOAc, precipitated with light petroleum and filtered.

1-(2-(Furan-2-yl)-5-(methylamino)-[1,2,4]triazolo[1,5-a][1,3,5]triazin-7-yl)-3-phenylurea *(11)*. White solid (15.8 mg, 15%); mp 194 °C; ^{1}H-NMR (DMSO-d$_6$) δ: 2.89 (d, *J*=4.4, 3H); 6.71 (s, 1H);

24

7.13-7.19 (m, 2H); 7.37 (t, J=7.6, 2H); 7.66 (d, J=7.6, 2H); 7.93 (s, 1H); 8.26 (bs, 1H); 10.24 (bs, 1H); 10.57 (s, 1H). IR (Nujol) cm^{-1}: 3044, 1718, 1633, 1614, 1538, 1513, 1486, 1407, 1396, 1308, 1241, 1185, 1107, 1011, 967, 773, 749, 700, 688, 627. Anal. ($C_{16}H_{14}N_8O_2$) C, H, N.

1-(2-(Furan-2-yl)-5-(isopropylamino)-[1,2,4]triazolo[1,5-a][1,3,5]triazin-7-yl)-3-phenylurea (**12**). Pale yellow solid (9 mg, 8%); mp 173°C; ^{1}H-NMR (DMSO-d$_6$) δ: 1.22 (s, 6H); 4.11 (bs, 1H); 6.71 (s, 1H); 7.13 (s, 2H); 7.38 (s, 2H); 7.63 (s, 2H); 7.92 (s, 1H); 8.18 (bs, 1H); 10.26 (bs, 1H); 10.46 (s, 1H). IR (Nujol) cm^{-1}: 3403, 1647, 1527, 1512, 1447, 1430, 1308, 1237, 1182, 1131, 1080, 1012, 968, 686. Anal. ($C_{18}H_{18}N_8O_2$) C, H, N.

1-(5-Cyclohexylamino-2-furan-2-yl-[1,2,4]triazolo[1,5-a][1,3,5]triazin-7-yl)-3-phenylurea (**13**). White solid (15 mg, 12%); mp 216 °C; ^{1}H-NMR (DMSO-d$_6$) δ: 1.14-1.31 (m, 5H); 1.61-1.98 (m, 5H); 3.77 (bs, 1H); 6.71 (s, 1H); 7.12 (bs, 2H); 7.37 (t, J=7.6, 2H); 7.64 (d, J=7.6, 2H); 7.92 (s, 1H); 8.16 (bs, 1H); 10.30 (bs, 1H); 10.43 (s, 1H). IR (Nujol) cm^{-1}: 3418, 2938, 2854, 1707, 1645, 1593, 1530, 1511, 1446, 1409, 1310, 1230, 1181, 1131, 1013, 968, 904, 884, 776, 746, 690. Anal. ($C_{21}H_{22}N_8O_2$) C, H, N.

1-(5-Benzylamino-2-furan-2-yl-[1,2,4]triazolo[1,5-a][1,3,5]triazin-7-yl)-3-phenylurea (**14**). Pale yellow solid (29 mg, 23%); mp 142 °C; ^{1}H-NMR (DMSO-d$_6$) δ: 4.59 (d, J=5, 2H); 6.71 (s, 1H); 7.12 (bs, 2H); 7.21-7.53 (m, 7H); 7.66 (d, J=7.7, 2H); 7.93 (s, 1H); 8.85 (bs, 1H);10.28 (bs, 1H); 10.58 (s, 1H). IR (Nujol) cm^{-1}: 3369, 1700, 1640, 1532, 1508, 1449, 1364, 1353, 1311, 1238, 1182, 1133, 1012, 970, 904, 777, 744, 700, 692. Anal. ($C_{22}H_{18}N_8O_2$) C, H, N.

General procedure for the synthesis of N-(2-(furan-2-yl)-5-(substitutedamino)-[1,2,4]triazolo[1,5-a][1,3,5]triazin-7-yl)benzamide (15-18) and N-(2-(furan-2-yl)-5-(substitutedamino)-[1,2,4]triazolo[1,5-a][1,3,5]triazin-7-yl)-2-phenylacetamide (19-22). 0.3 mmol of N^5-substituted-2-furan-2-yl-[1,2,4]triazolo[1,5-*a*][1,3,5]triazine-5,7-diamine (**7-10**) were dissolved in 5 mL of 1,4-dioxane, then 0.36 mmol of benzoylchloride (46 mg, 42 µL, for compounds **15-18**) or phenylacetylchloride (56 mg, 48 µL, for compounds **19-22**) and 0.36 mmol (36 mg, 50 µL) of TEA were added to the solution. Reaction was stirred under reflux for 24 h and then it was monitored by

TLC (EtOAc 3/ Light petroleum 7 or EtOAc 4/ Light petroleum 6). Reactions do not go to completion. The solvent was removed under reduced pressure; the residue was dissolved in dichloromethane and washed three times with water and brine. Organic layers were collected, dried on sodium sulfate anhydrous and the solvent was removed. The crude was purified by column chromatography (EtOAc/ Light petroleum mixtures) to give the desired compounds **15-22** that were further suspended in EtOAc and precipitated with light petroleum.

N-(2-(Furan-2-yl)-5-(methylamino)-[1,2,4]triazolo[1,5-a][1,3,5]triazin-7-yl)benzamide **(15)**. Column chromatography with gradient elution starting at EtOAc 3/ Light petroleum 7. White solid (23 mg, 23%); mp 233 °C; ^{1}H-NMR (DMSO-d_6) δ: 3.49 (s, 3H); 6.69 (s, 1H); 7.13 (s, 1H); 7.34-7.48 (m, 5H); 7.90 (s, 1H); 8.80 (bs, 1H); 8.89 (bs, 1H). IR (Nujol) cm^{-1}: 3397, 1689, 1644, 1604, 1573, 1506, 1430, 1418, 1372, 1341, 1318, 1241, 1220, 1180, 1119, 1040, 1013, 782, 730, 698. Anal. ($C_{16}H_{13}N_7O_2$) C, H, N.

N-(2-(Furan-2-yl)-5-(isopropylamino)-[1,2,4]triazolo[1,5-a][1,3,5]triazin-7-yl)benzamide **(16)**. Column chromatography with gradient elution starting at EtOAc 3/ Light petroleum 7. Pale yellow solid (33.8 mg, 31%); mp 110 °C; ^{1}H-NMR (DMSO-d_6) δ: 1.42 (d, *J*=5.6, 6H); 4.74-5.25 (m, 1H); 6.69 (s, 1H); 7.12 (s, 1H); 7.23-7.71 (m, 5H); 7.90 (s, 1H); 8.75 (bs, 1H); 8.83 (bs, 1H). IR (Nujol) cm^{-1}: 3424, 2988, 2927, 1654, 1560, 1512, 1448, 1404, 1270, 1178, 1126, 1078, 1015, 974, 781. Anal. ($C_{18}H_{17}N_7O_2$) C, H, N.

N-(5-(Cyclohexylamino)-2-(furan-2-yl)-[1,2,4]triazolo[1,5-a][1,3,5]triazin-7-yl)benzamide **(17)**. Column chromatography with gradient elution starting at EtOAc 2/ Light petroleum 8. White solid (33.9 mg, 28%); mp 220 °C; ^{1}H-NMR (DMSO-d_6) δ:

1.17-1.36 (m, 3H); 1.62-2.04 (m, 7H); 4.59 (bs, 1H); 6.69 (s, 1H); 7.13 (s, 1H); 7.33-7.50 (m, 5H); 7.90 (s, 1H); 8.77 (bs, 1H); 8.87 (bs, 1H). IR (Nujol) cm^{-1}: 3422, 2929, 2856, 1657, 1599, 1555, 1511, 1450, 1409, 1324, 1276, 1263, 1248, 1178, 1127, 1012, 906, 782, 733, 697. MS-ESI (MeOH): m/z = 404.3 (M+1); 426.3 (M+23); 442.4 (M+39). Anal. ($C_{21}H_{21}N_7O_2$) C, H, N.

N-(5-(Benzylamino)-2-(furan-2-yl)-[1,2,4]triazolo[1,5-a][1,3,5]triazin-7-yl)benzamide **(18)**.

Column chromatography with gradient elution starting at EtOAc 2/ Light petroleum 8. White solid (32 mg, 26%); mp 200 °C; ^{1}H-NMR (DMSO-d$_6$) δ: 5.26 (s, 2H); 6.69 (s, 1H); 7.12 (s, 1H); 7.17-7.71 (m, 10H); 7.90 (s, 1H); 8.82 (bs, 1H); 8.90 (bs, 1H). IR (Nujol) cm^{-1}: 3422, 1660, 1625, 1599, 1556, 1512, 1453, 1404, 1366, 1324, 1292, 1253, 1178, 1128, 1075, 1014, 970, 907, 782, 727, 699. Anal. (C$_{22}$H$_{17}$N$_7$O$_2$) C, H, N.

N-(2-(Furan-2-yl)-5-(methylamino)-[1,2,4]triazolo[1,5-a][1,3,5]triazin-7-yl)-2-phenylacetamide (19). 72h of reaction. Column chromatography with gradient elution starting at EtOAc 2/ Light petroleum 8. White solid (20 mg, 19%); mp> 250 °C; ^{1}H-NMR (DMSO-d$_6$) δ: 2.83 (s, 3H); 4.05 (s, 2H); 6.70 (s, 1H); 7.14 (s, 1H); 7.33 (s, 5H); 7.92 (s, 1H); 8.07 (bs, 1H); 11.22 (bs, 1H). IR (Nujol) cm^{-1}: 3431, 1654, 1636, 1618, 1542, 1508, 1459, 1404, 1342, 1303, 1270, 1214, 1178, 1110, 1008, 972, 903, 882, 776, 701, 686. Anal. (C$_{17}$H$_{15}$N$_7$O$_2$) C, H, N.

N-(2-(Furan-2-yl)-5-(isopropylamino)-[1,2,4]triazolo[1,5-a][1,3,5]triazin-7-yl)-2-phenylacetamide (20). Column chromatography with gradient elution starting at EtOAc 4/ Light petroleum 6. White solid (31 mg, 27%); mp 189 °C; ^{1}H-NMR (DMSO-d$_6$) δ: 1.17 (d, *J*=6.3, 6H); 3.90-4.31 (m, 3H); 6.71 (s, 1H); 7.13 (s, 1H); 7.19-7.41 (m, 5H); 7.92 (s, 1H); 8.02 (d, *J*=7.8, 1H); 11.27 (bs, 1H). IR (Nujol) cm^{-1}: 3404, 2973, 2933, 1736, 1646, 1619, 1588, 1542, 1522, 1432, 1413, 1388, 1366, 1341, 1314, 1265, 1224, 1178, 1136, 1104, 1076, 1031, 1014, 975, 905, 884, 861, 780, 734, 700. Anal. (C$_{19}$H$_{19}$N$_7$O$_2$) C, H, N.

N-(5-(Cyclohexylamino)-2-(furan-2-yl)-[1,2,4]triazolo[1,5-a][1,3,5]triazin-7-yl)-2-phenylacetamide (21). Column chromatography with gradient elution starting at EtOAc 3/ Light petroleum 7. Yellow solid (42 mg, 34%); mp 200 °C; ^{1}H-NMR (DMSO-d$_6$) δ: 1.13-1.28 (m, 5H); 1.57-1.88 (m, 5H); 3.74 (bs, 1H); 4.05 (bs, 2H); 6.71 (s, 1H); 7.13 (s, 1H); 7.33 (bs, 5H); 7.92 (s, 1H); 8.06 (d, *J*=7.4, 1H); 11.20 (bs, 1H). IR (Nujol) cm^{-1}: 3392, 2927, 2909, 1740, 1646, 1618, 1590, 1560, 1540, 1522, 1496, 1458, 1406, 1360, 1307, 1262, 1226, 1178, 1163, 1144, 1106, 1050, 1010, 968, 826, 779, 754, 742, 704, 680, 664. Anal. (C$_{22}$H$_{23}$N$_7$O$_2$) C, H, N.

N-(5-(Benzylamino)-2-(furan-2-yl)-[1,2,4]triazolo[1,5-a][1,3,5]triazin-7-yl)-2-phenylacetamide

27

(22). Column chromatography with gradient elution starting at EtOAc 3/ Light petroleum 7. Yellow solid (25.5 mg, 20%); mp 145 °C; ^{1}H-NMR (acetone-d$_6$) δ: 4.31 (s, 2H); 4.73 (t, *J*=7.2, 2H); 6.65 (m, 1H); 7.12 (d, *J*=3.2, 1H); 7.21-7.65 (m, 10H); 7.79 (s, 1H); 7.87 (bs, 1H); 9.75 (bs, 1H). IR (Nujol) cm^{-1}: 3420, 2355, 1734, 1644, 1620, 1539, 1520, 1496, 1454, 1420, 1388, 1360, 1314, 1267, 1220, 1159, 1134, 1106, 1098, 1075, 1028, 1013, 973, 905, 884, 779, 742, 700. Anal. (C$_{23}$H$_{19}$N$_7$O$_2$) C, H, N.

General procedure for the synthesis of N-alkyl-2-(furan-2-yl)-5-phenoxy-[1,2,4]triazolo[1,5-a][1,3,5]triazin-7-amine (23-25) and N5,N7-di(4-fluorobenzyl)-2-(furan-2-yl)-[1,2,4]triazolo[1,5-a][1,3,5]triazin-5,7-diamine (37). 500 mg of compound **5** (1.348 mmol) were dissolved in 10 mL of ethanol. 1.348 mmol of the desired amine were added to the solution and the reaction was stirred at 60°C for 3 hours. The reaction was monitored by TLC (EtOAc 3/ Light petroleum 7). When the starting material was disappeared, the solvent was removed and the crude purified by column chromatography with gradient elution starting at EtOAc 2/ Light petroleum 8.

N-Cyclohexyl-2-(furan-2-yl)-5-phenoxy-[1,2,4]triazolo[1,5-a][1,3,5]triazin-7-amine (23). White solid (264 mg, 52%); mp 178 °C; ^{1}H-NMR (DMSO-d$_6$) δ: 0.94-1.41 (m, 3H); 1.41-1.95 (m, 7H); 3.86 (bs, 1H); 6.69 (dd, *J*=3.2, *J*=1.8, 1H); 7.12 (d, *J*=3.2, 1H); 7.19-7.38 (m, 3H); 7.46 (t, *J*=7.6, 2H); 7.91 (s, 1H); 9.25 (bs, 1H). IR (Nujol) cm^{-1}: 3388, 2930, 2856, 2362, 2057, 1640, 1603, 1560, 1522, 1511, 1490, 1451, 1418, 1385, 1321, 1294, 1228, 1186, 1128, 1073, 1060, 1012, 974, 906, 885, 779, 754, 740, 690, 650. Anal. (C$_{20}$H$_{20}$N$_6$O$_2$) C, H, N.

N-Benzyl-2-(furan-2-yl)-5-phenoxy-[1,2,4]triazolo[1,5-a][1,3,5]triazin-7-amine (24). White solid (170 mg, 33%); mp 190 °C; ^{1}H-NMR (CDCl$_3$) δ: 4.78 (d, *J*=5.8, 2H); 6.55 (dd, *J*=3.4, *J*=1.8, 1H); 6.86 (bs, 1H); 7.05-7.53 (m, 10H); 7.56 (s, 1H). IR (Nujol) cm^{-1}: 3470, 1636, 1618, 1604, 1570, 1559, 1540, 1522, 1490, 1456, 1414, 1388, 1362, 1306, 1229, 1177, 1131, 1065, 1022, 968, 907, 834, 778, 754, 704, 680, 663, 650, 634, 622. Anal. (C$_{21}$H$_{16}$N$_6$O$_2$) C, H, N.

N-(4-Fluorobenzyl)-2-(furan-2-yl)-5-phenoxy-[1,2,4]triazolo[1,5-a][1,3,5]triazin-7-amine (25). From 1.26 g of compound **5** (3.39 mmol) and 388 µL of 4-fluorobenzylamine (425 mg, 3.39 mmol).

28

White solid (140 mg, 10%); mp 201 °C; ^{1}H-NMR (DMSO-d$_6$) δ: 4.53 (s, 2H); 6.70 (s, 1H); 6.88-7.36 (m, 8H); 7.36-7.68 (m, 2H); 7.92 (s, 1H); 9.91 (bs, 1H). IR (Nujol) cm^{-1}: 3392, 1643, 1604, 1587, 1510, 1489, 1416, 1224, 778, 750. Anal. (C$_{21}$H$_{15}$FN$_6$O$_2$) C, H, N. Further elution of the column with EtOAc 9/light petroleum 1 gave N5,N7-di(4-fluorobenzyl)-2-(furan-2-yl)-[1,2,4]triazolo[1,5-*a*][1,3,5]triazin-5,7-diamine (**37**). White solid (120 mg, 16%); mp 193 °C; ^{1}H-NMR (DMSO-d$_6$) δ: 4.47 (d, *J*=5.3, 2H); 4.58 (d, *J*=6.8, 2H); 6.66 (dd, *J*=3.4, *J*=1.8, 1H); 6.84-7.22 (m, 4H); 7.22-7.61 (m, 4H); 7.86 (s, 1H); 8.14 (bs, 1H); 9.18 (bs, 1H). IR (Nujol) cm^{-1}: 3449, 1633, 1613, 1556, 1563, 1494, 1412, 1306, 1222, 778, 737. Anal. (C$_{22}$H$_{18}$FN$_7$O) C, H, N.

Procedure for the synthesis of N5,N7-dicyclohexyl-2-(furan-2-yl)-[1,2,4]triazolo[1,5-a][1,3,5]triazin-5,7-diamine (28). 500 mg of compound **5** (1.348 mmol) were dissolved in 10 mL of ethanol. 0.46 mL of cyclohexylamine (401 mg, 4.043 mmol) were added to the solution and the reaction was stirred at reflux for 3 hours. The reaction was monitored by TLC (EtOAc 3/ light petroleum 7). When the starting material was disappeared, the solvent was removed and the crude purified by column chromatography with gradient elution starting at EtOAc 2/ Light petroleum 8 to provide 95 mg of compound **23** (18.7%) and 53 mg of the desired compound **28** (white solid, 10%). Compound **28**: mp 205 °C. ^{1}H-NMR (CDCl3) δ: 1.02-1.55 (m, 10H); 1.55-1.95 (m, 6H); 1.95-2.27 (m, 4H); 3.95 (bs, 1H); 5.14 (d, *J*=8, 1H); 6.02 (d, *J*=8.1, 1H); 6.54 (dd, *J*=1.7, *J*=3.3, 1H); 7.18 (d, *J*=3.3, 1H); 7.56 (s, 1H). IR (Nujol) cm^{-1}: 3402, 2925, 2850, 1641, 1597, 1559, 1488, 1432, 1181, 779, 737. Anal. (C$_{20}$H$_{27}$N$_7$O) C, H, N.

Procedure for the synthesis of N5,N7-dibenzxyl-2-(furan-2-yl)-[1,2,4]triazolo[1,5-a][1,3,5]triazin-5,7-diamine (33). 50 mg of compound **5** (0.135 mmol) were dissolved in 2 mL of ethanol. 74 µL of benzylamine (72 mg, 0.674 mmol) were added to the solution and the reaction was stirred at 120 °C in a sealed tube for 3 hours. The reaction was monitored by TLC (EtOAc 1/ Light petroleum 1). When the starting material was disappeared, the solvent was removed and the crude purified by column chromatography with gradient elution starting at EtOAc 1/ Light petroleum 1 to provide 37 mg of the desired compound **33** (white solid, 70%). Mp 148 °C. ^{1}H-NMR (DMSO-d$_6$) δ: 4.48-4.62

29

(m, 4H); 6.67 (s, 1H); 7.06 (s, 1H); 7.13-7.59 (m, 10H); 7.87 (s, 1H); 8.16 (bs, 1H); 9.14 (bs, 1H). IR (Nujol) cm^{-1}: 3414, 1644, 1496, 1421, 1306, 1182, 778, 735, 697. Anal. (C$_{22}$H$_{19}$N$_7$O) C, H, N.

General procedure for the synthesis of N5,N7-disubstituted-2-(furan-2-yl)-[1,2,4]triazolo[1,5-a][1,3,5]triazin-5,7-diamine (26,27,29-32,34-36)*.* 45-73 mg of compounds **23-25** were dissolved in 2-4 mL of ethanol. 1.1-4.5 eq of the desired amine were added to the solution and the reaction was stirred at 70-100°C from 24 to 72 hours. The solvent was then removed, and the crude was purified by column chromatography (EtOAc/ Light petroleum mixtures). The obtained solid was dissolved in EtOAc and precipitated with light petroleum providing the desired compound as a solid (**26,27,29-32,34-36**).

*N7-Cyclohexyl-2-(furan-2-yl)-N5-methyl-[1,2,4]triazolo[1,5-a][1,3,5]triazine-5,7-diamine (**26**).* 50 mg of compound **23** (0.133 mmol) were reacted with 66 µL of methylamine 33 wt. % solution in ethanol (50 mg, 0.532 mmol) at 70 °C for 72 hours. Column chromatography with gradient elution starting at EtOAc 6/ Light petroleum 4. Pale yellow solid (26 mg, 63%); mp 114 °C; ^{1}H-NMR (DMSO-d$_6$) δ: 0.96-1.40 (m, 3H); 1.40-1.69 (m, 3H); 1.80 (t, *J*=12,3, 4H); 2.79 (d, *J*=4, 3H); 3.94 (bs, 1H); 6.67 (s, 1H); 7.05 (s, 1H); 7.49 (d, *J*=4, 1H); 7.87 (s, 1H); 8.31 (d, *J*=8.3, 1H). IR (Nujol) cm^{-1}: 3378, 2937, 2850, 1643, 1600, 1566, 1504, 1412, 1180, 779, 739. Anal. (C$_{15}$H$_{19}$N$_7$O) C, H, N.

*N7-Cyclohexyl-2-(furan-2-yl)-N5-isopropyl-[1,2,4]triazolo[1,5-a][1,3,5]triazine-5,7-diamine (**27**).* 70 mg of compound **23** (0.186 mmol) were reacted with 48 µL of isopropylamine (33 mg, 0.558 mmol) at 70 °C for 24 hours. Column chromatography with gradient elution starting at EtOAc 0.4/ Dichloromethane 9.6. White solid (26 mg, 55%); mp 134 °C; ^{1}H-NMR (CD$_3$OD) δ: 1.27 (d, *J*=6.5, 6H); 1.34-1.59 (m, 4H); 1.59-1.94 (m, 4H); 2.03 (bs, 2H); 4.02 (bs, 1H); 4.12-4.22 (m, 1H); 6.61 (dd, *J*=1.8, *J*=3.4, 1H); 7.11 (d, *J*=3.4, 1H); 7.69 (d, J = 0.8 Hz, 1H). IR (Nujol) cm^{-1}: 3394, 2930, 2849, 1642, 1600, 1562, 1489, 1414, 1180, 780, 737. Anal. (C$_{17}$H$_{23}$N$_7$O) C, H, N.

*N5-Benzyl-N7-cyclohexyl-2-(furan-2-yl)-[1,2,4]triazolo[1,5-a][1,3,5]triazine-5,7-diamine (**29**).* 73 mg of compound **23** (0.194 mmol) were reacted with 23 µL of benzylamine (23 mg, 0.213 mmol) at 70 °C for 72 hours. Column chromatography with gradient elution starting at EtOAc 3/ Light

petroleum 7. White solid (50 mg, 67%); mp 231 °C; ^{1}H-NMR (DMSO-d$_6$) δ: 0.88-1.94 (m, 10H); 3.94 (bs, 1H); 4.48 (d, *J*=5.8, 2H); 6.67 (bs, 1H); 7.04 (d, *J*=3.2, 1H); 7.11-7.57 (m, 5H); 7.86 (s, 1H); 7.99-8.30 (m, 1H); 8.41 (d, *J*=8.3, 1H). IR (Nujol) cm^{-1}: 3402, 2923, 2848, 1635, 1614, 1574, 1494, 1421, 1318, 1182, 779, 731, 708, 695. Anal. (C$_{21}$H$_{23}$N$_7$O) C, H, N.

N7-Benzyl-2-(furan-2-yl)-N5-methyl-[1,2,4]triazolo[1,5-a][1,3,5]triazine-5,7-diamine (30). 50 mg of compound **24** (0.130 mmol) were reacted with 48 µL of methylamine 33 wt. % solution in ethanol (37 mg, 0.390 mmol) at 80 °C for 24 hours. Column chromatography with gradient elution starting at EtOAc 3/ light petroleum 7. White solid (27 mg, 65%); mp 193 °C; ^{1}H-NMR (DMSO-d$_6$) δ: 2.80 (s, 3H); 4.62 (s, 2H); 6.68 (s, 1H); 7.06 (s, 1H); 7.15-7.71 (m, 6H); 7.87 (s, 1H); 9.11 (s, 1H). IR (Nujol) cm^{-1}:3450, 1644, 1611, 1570, 1500, 1413, 778, 737, 696. Anal. (C$_{16}$H$_{15}$N$_7$O) C, H, N.

N7-Benzyl-2-(furan-2-yl)-N5-isopropyl-[1,2,4]triazolo[1,5-a][1,3,5]triazine-5,7-diamine (31). 98 mg of compound **24** (0.254 mmol) were reacted with 66 µL of isopropylamine (45 mg, 0.762 mmol) at 70 °C for 24 hours. Column chromatography in aluminum oxide grade III with gradient elution starting at EtOAc 4/ Light petroleum 6. White solid (37 mg, 42%); mp 191 °C; ^{1}H-NMR (DMSO-d$_6$) δ: 1.13 (d, *J*=5.4, 6H); 3.79-4.27 (m, 1H); 4.62 (s, 2H); 6.67 (s, 1H); 7.06 (s, 1H); 7.17-7.71 (m, 6H); 7.87 (s, 1H); 9.10 (bs, 1H). IR (Nujol) cm^{-1}: 3402, 2970, 2923, 1643, 1602, 1566, 1493, 1432, 1317, 1180, 780, 738, 697. Anal. (C$_{18}$H$_{19}$N$_7$O) C, H, N.

N7-Benzyl-N5-cyclohexyl-2-(furan-2-yl)-[1,2,4]triazolo[1,5-a][1,3,5]triazine-5,7-diamine (32). 50 mg of compound **24** (0.130 mmol) were reacted with 45 µL of cyclohexylamine (39 mg, 0.390 mmol) at 70 °C for 24 hours. Column chromatography with gradient elution starting at EtOAc 3/ Light petroleum 7. White solid (25 mg, 53%); mp 122 °C; ^{1}H-NMR (DMSO-d$_6$) δ: 0.84-1.41 (m, 5H); 1.57-1.88 (m, 5H); 3.69 (bs, 1H); 4.60 (d, *J*=9.6, 2H); 6.68 (s, 1H); 7.05 (s, 1H); 7.23-7.53 (m, 6H); 7.87 (s, 1H); 9.07 (bs, 1H). IR (Nujol) cm^{-1}: 3432, 2925, 2848, 1644, 1488, 1431, 1316, 1180, 778, 736. Anal. (C$_{21}$H$_{23}$N$_7$O) C, H, N.

N7-(4-Fluorobenzyl)-2-(furan-2-yl)-N5-methyl-[1,2,4]triazolo[1,5-a][1,3,5]triazine-5,7-diamine

(34). 45 mg of compound **25** (0.112 mmol) were reacted with 63 µL of methylamine 33 wt. %

31

solution in ethanol (47 mg, 0.504 mmol) at 90 °C for 48 hours. Column chromatography with gradient elution starting at EtOAc 3/ Light petroleum 7. White solid (25 mg, 66%); mp 126 °C; ^{1}H-NMR (DMSO-d_6) δ: 2.80 (d, *J*=4.1, 3H); 4.59 (s, 2H); 6.67 (s, 1H); 7.04-7.19 (m, 3H); 7.41-7.48 (m, 3H); 7.86 (s, 1H); 9.08 (bs, 1H). IR (Nujol) cm^{-1}: 3444, 1653, 1644, 1507, 1456, 1412, 1218, 1124, 1009, 735. Anal. ($C_{16}H_{14}FN_7O$) C, H, N.

N5-Cyclohexyl-N7-(4-fluorobenzyl)-2-(furan-2-yl)-[1,2,4]triazolo[1,5-a][1,3,5]triazine-5,7-diamine (35). 45 mg of compound **25** (0.112 mmol) were reacted with 35 µL of cyclohexylamine (28 mg, 0.280 mmol) at 100 °C for 48 hours. Column chromatography with gradient elution starting at EtOAc 3/ Light petroleum 7. White solid (30 mg, 67%); mp 127 °C; ^{1}H-NMR (DMSO-d_6) δ: 0.92-1.48 (m, 5H); 1.50-2.13 (m, 5H); 3.70 (bs, 1H); 4.59 (s, 2H); 6.67 (s, 1H); 6.90-7.19 (m, 3H); 7.33-7.74 (m, 3H); 7.86 (s, 1H); 9.04 (s, 1H). IR (Nujol) cm^{-1}: 3429, 2926, 2850, 1642, 1608, 1570, 1509, 1488, 1415, 1314, 1220, 1181, 779, 739. Anal. ($C_{21}H_{22}FN_7O$) C, H, N.

N5-Benzyl-N7-(4-fluorobenzyl)-2-(furan-2-yl)-[1,2,4]triazolo[1,5-a][1,3,5]triazine-5,7-diamine (36). 45 mg of compound **25** (0.112 mmol) were reacted with 30 µL of benzylamine (30 mg, 0.280 mmol) at 100 °C for 48 hours. Column chromatography with gradient elution starting at EtOAc 3/ Light petroleum 7. White solid (19 mg, 41%); mp 174 °C; ^{1}H-NMR (DMSO-d_6) δ: 4.28-480 (m, 4H); 6.67 (s, 1H); 6.85-7.68 (m, 10H); 8.86 (s, 1H); 8.14 (bs, 1H); 9.18 (bs, 1H). IR (Nujol) cm^{-1}: 3424, 1644, 1623, 1612, 1570, 1507, 1497, 1420, 1306, 1221, 1182, 779, 736, 697. Anal. ($C_{22}H_{18}FN_7O$) C, H, N.

4.2 Biological activity.

Binding at human A_1, A_{2A} and A_3 ARs. All pharmacological methods followed the procedures as described earlier[32]. In brief, membranes for radioligand binding were prepared from CHO cells stably transfected with hAR subtypes in a two-step procedure. In a first step cell fragments and nuclei were removed at 1,000 x g and then the crude membrane fraction was sedimented from the supernatant at 100,000 x g. The membrane pellet was resuspended in the buffer used for the respective binding experiments, frozen in liquid nitrogen and stored at 80 °C. For radioligand

binding at the hA$_1$ AR 1 nM [^{3}H]CCPA was used, whereas 10 nM [^{3}H]NECA was used for h A$_{2A}$ and 1 nM [^{3}H]HEMADO was used for hA$_3$ AR binding. Non specific binding of [^{3}H]CCPA was determined in the presence of 1 mM theophylline, in the case of [^{3}H]NECA and [^{3}H]HEMADO 100 μM R-PIA was used[33]. K$_i$ values from competition experiments were calculated with the program SCTFIT.

Adenylyl cyclase activity. The potency of antagonists at the hA$_{2B}$ AR was determined in adenylyl cyclase experiments. The procedure was carried out as described previously with minor modifications[32,34]. Membranes were prepared from CHO cells stably transfected with hA$_{2B}$ ARs by only one high speed centrifugation of the homogenate. The resulting crude membrane pellet was resuspended in 50 mM Tris/HCl, pH 7.4 and immediately used for the cyclase assay. Membranes were incubated with about 150,000 cpm of [α-^{32}P]ATP for 20 min in the incubation mixture as described without EDTA and NaCl[34,35]. The IC$_{50}$-values for concentration-dependent inhibition of NECA-stimulated adenylyl cyclase caused by antagonists were calculated with the Hill equation. Hill coefficients in all experiments were near unity.

4.3 Molecular Modelling

Energy computation and analyses of docking poses were performed using the MOE[36] suite (Molecular Operating Environment, version 2014.09). Docking simulations were carried out with the GOLD[37] (Genetic Optimization for Ligand Docking, version 5.2) suite.

Three-Dimensional Structures of hARs. Among all the currently available crystallographic structures of hA$_{2A}$ AR, we selected for our docking simulations a complex with the selective and high affinity inverse agonist ZM 241385. Among the structures co-crystallized with ZM 241385, we selected the one with the highest resolution and fewest missing atoms (PDB code: 4EIY, 1.80 Å resolution)[38]. As, to date, no crystallographic information about all other AR subtypes are available, we used a previously build homology models deposited in our web platform dedicated to ARs, *Adenosiland*[39,40]. The numbering of the amino acids follows the arbitrary scheme proposed by

Ballesteros and Weinstein[41]: each amino acid identifier starts with the helix number (1–7), followed by a dot and the position relative to a reference residue among the most conserved amino acids in that helix, to which the number 50 is arbitrarily assigned.

Molecular Docking. Ligand structures were built using the MOE-builder tool, as part of the MOE suite[36], and were subjected to a MMFF94x energy minimization until the rms conjugate gradient was <0.05 kcal mol^{-1} Å^{-1}. We used the Protonate 3D[42] methodology, part of the MOE suite, for protonation state assignments. According to the docking benchmark study we have previously conducted[43], docking simulations were performed with the docking tool of GOLD[37] suite as conformational search program and the GoldScore as scoring function. For each selected compound, 20 independent docking runs were performed and searching was conducted within a user-specified docking sphere (20 Å radius and centered on the barycenter of the Asn(6.55) residue). Electrostatic and hydrophobic contributions to the binding energy of individual receptor residues have been calculated using the MOE[36] suite (see below). To estimate the electrostatic contributions, atomic partial charges for the ligands were calculated using PM3/ESP methodology. Partial charges for protein amino acids were calculated with the AMBER99 force field.

Interaction Energy Fingerprints (IEFs). Individual electrostatic and hydrophobic contributions to the interaction energy (hereby denoted as IEele and IEhyd, respectively) of each receptor residue involved in the binding with the ligand were computed with the MOE[36] suite . In particular, the IEele was computed on the basis of the nonbonded electrostatic interaction energy term of the force field, whereas the IEhyd contributions was calculated by using the directional hydrophobic interaction term based on contact surfaces as implemented in the MOE[36] scoring function. IEele values are expressed in kcal/mol, whereas IEhyd values are reported as adimensional scores (the higher the better). The IEFs analysis are graphically transferred either into colored maps or into histograms reporting the key residues involved in the binding with the considered ligands along with a quantitative estimate of the occurring interactions.

34

REFERENCES

(1) Chen, J.-F.; Eltzschig, H. K.; Fredholm, B. B. Adenosine Receptors as Drug Targets — What Are the Challenges? *Nat. Rev. Drug Discov.* **2013**, *12* (4), 265–286.

(2) Downey, J. M.; Cohen, M. V.; Ytrehus, K.; Liu, Y. Cellular Mechanisms in Ischemic Preconditioning: The Role of Adenosine and Protein Kinase C. *Ann. N. Y. Acad. Sci.* **1994**, *723* (1 Cellular, Bio), 82–98.

(3) Auchampach, J. A.; Jin, X.; Wan, T. C.; Caughey, G. H.; Linden, J. Canine Mast Cell Adenosine Receptors: Cloning and Expression of the A3 Receptor and Evidence That Degranulation Is Mediated by the A2B Receptor. *Mol. Pharmacol.* **1997**, *52* (5), 846–860.

(4) Mustafa, S. J.; Morrison, R. R.; Teng, B.; Pelleg, A. Adenosine Receptors and the Heart: Role in Regulation of Coronary Blood Flow and Cardiac Electrophysiology. In *Adenosine Receptors in Health and Disease*; Wilson, C. N., Mustafa, S. J., Eds.; Springer Berlin Heidelberg: Berlin, Heidelberg, 2009; Vol. 193, pp 161–188.

(5) Headrick, J. P.; Ashton, K. J.; Rose'Meyer, R. B.; Peart, J. N. Cardiovascular Adenosine Receptors: Expression, Actions and Interactions. *Pharmacol. Ther.* **2013**, *140* (1), 92–111.

(6) Gomes, C. V.; Kaster, M. P.; Tomé, A. R.; Agostinho, P. M.; Cunha, R. A. Adenosine Receptors and Brain Diseases: Neuroprotection and Neurodegeneration. *Biochim. Biophys. Acta BBA - Biomembr.* **2011**, *1808* (5), 1380–1399.

(7)   Stone, T. W.; Ceruti, S.; Abbracchio, M. P. Adenosine Receptors and Neurological Disease: Neuroprotection and Neurodegeneration. In *Adenosine Receptors in Health and Disease*; Wilson, C. N., Mustafa, S. J., Eds.; Springer Berlin Heidelberg: Berlin, Heidelberg, 2009; Vol. 193, pp 535–587.

(8)   Polosa, R.; Blackburn, M. R. Adenosine Receptors as Targets for Therapeutic Intervention in Asthma and Chronic Obstructive Pulmonary Disease. *Trends Pharmacol. Sci.* **2009**, *30* (10), 528–535.

(9)   Wilson, C. N. Adenosine Receptors and Asthma in Humans: Adenosine Receptors and Asthma in Humans. *Br. J. Pharmacol.* **2009**, *155* (4), 475–486.

(10)   Richardson, P. J.; Kase, H.; Jenner, P. G. Adenosine A2A Receptor Antagonists as New Agents for the Treatment of Parkinson's Disease. *Trends Pharmacol. Sci.* **1997**, *18* (9), 338–344.

(11)   Müller, C. E.; Jacobson, K. A. Recent Developments in Adenosine Receptor Ligands and Their Potential as Novel Drugs. *Biochim. Biophys. Acta BBA - Biomembr.* **2011**, *1808* (5), 1290–1308.

(12)   Baraldi, P. G.; Cacciari, B.; Spalluto, G.; Pineda de las Infantas y Villatoro, M. J.; Zocchi, C.; Dionisotti, S.; Ongini, E. Pyrazolo[4,3- *e*]-1,2,4-triazolo[1,5- *c*]pyrimidine Derivatives: Potent and Selective A $_{2A}$ Adenosine Antagonists. *J. Med. Chem.* **1996**, *39* (5), 1164–1171.

(13)   Baraldi, P. G.; Cacciari, B.; Spalluto, G.; Bergonzoni, M.; Dionisotti, S.; Ongini, E.; Varani, K.; Borea, P. A. Design, Synthesis, and Biological Evaluation of a Second Generation of Pyrazolo[4,3- *e*]-1,2,4-triazolo[1,5- *c*]pyrimidines as Potent and Selective A $_{2A}$ Adenosine Receptor Antagonists. *J. Med. Chem.* **1998**, *41* (12), 2126–2133.

(14)   Baraldi, P. G.; Cacciari, B.; Romagnoli, R.; Spalluto, G.; Klotz, K.-N.; Leung, E.; Varani, K.; Gessi, S.; Merighi, S.; Borea, P. A. Pyrazolo[4,3- *e*]-1,2,4-triazolo[1,5- *c*]pyrimidine Derivatives as Highly Potent and Selective Human A $_3$ Adenosine Receptor Antagonists. *J. Med. Chem.* **1999**, *42* (22), 4473–4478.

(15) Baraldi, P. G.; Cacciari, B.; Romagnoli, R.; Spalluto, G.; Moro, S.; Klotz, K.-N.; Leung, E.; Varani, K.; Gessi, S.; Merighi, S.; Borea, P. A. Pyrazolo[4,3- *e*]1,2,4-triazolo[1,5- *c*]pyrimidine Derivatives as Highly Potent and Selective Human A $_3$ Adenosine Receptor Antagonists: Influence of the Chain at the N ^{8} Pyrazole Nitrogen. *J. Med. Chem.* **2000**, *43* (25), 4768–4780.

(16) Baraldi, P. G.; Cacciari, B.; Moro, S.; Spalluto, G.; Pastorin, G.; Da Ros, T.; Klotz, K.-N.; Varani, K.; Gessi, S.; Borea, P. A. Synthesis, Biological Activity, and Molecular Modeling Investigation of New Pyrazolo[4,3- *e*]-1,2,4-triazolo[1,5- *c*]pyrimidine Derivatives as Human A $_3$ Adenosine Receptor Antagonists. *J. Med. Chem.* **2002**, *45* (4), 770–780.

(17) Baraldi, P. G.; Cacciari, B.; Romagnoli, R.; Spalluto, G.; Monopoli, A.; Ongini, E.; Varani, K.; Borea, P. A. 7-Substituted 5-Amino-2-(2-furyl)pyrazolo[4,3- *e*]-1,2,4-triazolo[1,5- *c*]pyrimidines as A $_{2A}$ Adenosine Receptor Antagonists: A Study on the Importance of Modifications at the Side Chain on the Activity and Solubility. *J. Med. Chem.* **2002**, *45* (1), 115–126.

(18) Maconi, A.; Pastorin, G.; Da Ros, T.; Spalluto, G.; Gao, Z.; Jacobson, K. A.; Baraldi, P. G.; Cacciari, B.; Varani, K.; Moro, S.; Borea, P. A. Synthesis, Biological Properties, and Molecular Modeling Investigation of the First Potent, Selective, and Water-Soluble Human A $_3$ Adenosine Receptor Antagonist. *J. Med. Chem.* **2002**, *45* (17), 3579–3582.

(19) Pastorin, G.; Da Ros, T.; Spalluto, G.; Deflorian, F.; Moro, S.; Cacciari, B.; Baraldi, P. G.; Gessi, S.; Varani, K.; Borea, P. A. Pyrazolo[4,3- *e*]-1,2,4-triazolo[1,5- *c*]pyrimidine Derivatives as Adenosine Receptor Antagonists. Influence of the N5 Substituent on the Affinity at the Human A $_3$ and A $_{2B}$ Adenosine Receptor Subtypes: A Molecular Modeling Investigation. *J. Med. Chem.* **2003**, *46* (20), 4287–4296.

(20) Pastorin, G.; Da Ros, T.; Bolcato, C.; Montopoli, C.; Moro, S.; Cacciari, B.; Baraldi, P. G.; Varani, K.; Borea, P. A.; Spalluto, G. Synthesis and Biological Studies of a New Series of 5-heteroarylcarbamoylaminopyrazolo[4,3-e]1,2,4-triazolo[1,5-C]pyrimidines as Human A3

37

Adenosine Receptor Antagonists. Influence of the Heteroaryl Substituent on Binding Affinity and Molecular Modeling Investigations. *J. Med. Chem.* **2006**, *49* (5), 1720–1729.

(21) Cheong, S. L.; Dolzhenko, A.; Kachler, S.; Paoletta, S.; Federico, S.; Cacciari, B.; Dolzhenko, A.; Klotz, K.-N.; Moro, S.; Spalluto, G.; Pastorin, G. The Significance of 2-Furyl Ring Substitution with a 2-(*para* -Substituted) Aryl Group in a New Series of Pyrazolo-Triazolo-Pyrimidines as Potent and Highly Selective hA $_3$ Adenosine Receptors Antagonists: New Insights into Structure–Affinity Relationship and Receptor–Antagonist Recognition. *J. Med. Chem.* **2010**, *53* (8), 3361–3375.

(22) Federico, S.; Paoletta, S.; Cheong, S. L.; Pastorin, G.; Cacciari, B.; Stragliotto, S.; Klotz, K. N.; Siegel, J.; Gao, Z.-G.; Jacobson, K. A.; Moro, S.; Spalluto, G. Synthesis and Biological Evaluation of a New Series of 1,2,4-Triazolo[1,5- *a*]-1,3,5-Triazines as Human A $_{2A}$ Adenosine Receptor Antagonists with Improved Water Solubility. *J. Med. Chem.* **2011**, *54* (3), 877–889.

(23) Federico, S.; Ciancetta, A.; Sabbadin, D.; Paoletta, S.; Pastorin, G.; Cacciari, B.; Klotz, K. N.; Moro, S.; Spalluto, G. Exploring the Directionality of 5-Substitutions in a New Series of 5-Alkylaminopyrazolo[4,3- *e*]1,2,4-triazolo[1,5- *c*]pyrimidine as a Strategy To Design Novel Human A $_3$ Adenosine Receptor Antagonists. *J. Med. Chem.* **2012**, *55* (22), 9654–9668.

(24) Federico, S.; Ciancetta, A.; Porta, N.; Redenti, S.; Pastorin, G.; Cacciari, B.; Klotz, K. N.; Moro, S.; Spalluto, G. Scaffold Decoration at Positions 5 and 8 of 1,2,4-Triazolo[1,5-*c*]Pyrimidines to Explore the Antagonist Profiling on Adenosine Receptors: A Preliminary Structure–Activity Relationship Study. *J. Med. Chem.* **2014**, *57* (14), 6210–6225.

(25) Pastorin, G.; Federico, S.; Paoletta, S.; Corradino, M.; Cateni, F.; Cacciari, B.; Klotz, K.-N.; Gao, Z.-G.; Jacobson, K. A.; Spalluto, G.; Moro, S. Synthesis and Pharmacological Characterization of a New Series of 5,7-Disubstituted-[1,2,4]triazolo[1,5-a][1,3,5]triazine Derivatives as Adenosine Receptor Antagonists: A Preliminary Inspection of Ligand–receptor Recognition Process. *Bioorg. Med. Chem.* **2010**, *18* (7), 2524–2536.

(26) Poucher, S. M.; Keddie, J. R.; Singh, P.; Stoggall, S. M.; Caulkett, P. W. R.; Jones, G.; Collis, M. G. The in Vitro Pharmacology of ZM 241385, a Potent, Non-Xanthine, A2a Selective Adenosine Receptor Antagonist. *Br. J. Pharmacol.* **1995**, *115* (6), 1096–1102.

(27) De Zwart, M.; Vollinga, R. C.; Beukers, M. W.; Sleegers, D. F.; von Frijtag Drabbe Künzel, J. K.; de Groote, M.; Ijzerman, A. P. Potent Antagonists for the Human Adenosine A2B Receptor. Derivatives of the Triazolotriazine Adenosine Receptor Antagonist ZM241385 with High Affinity. *Drug Dev. Res.* **1999**, *48* (3), 95–103.

(28) Ji, X. D.; Jacobson, K. A. Use of the Triazolotriazine [3H]ZM 241385 as a Radioligand at Recombinant Human A2B Adenosine Receptors. *Drug Des. Discov.* **1999**, *16* (3), 217–226.

(29) Caulkett, P. W. R.; Jones, G.; McPartlin, M.; Renshaw, N. D.; Stewart, S. K.; Wright, B. Adenine Isosteres with Bridgehead Nitrogen. Part 1. Two Independent Syntheses of the [1,2,4]triazolo[1,5-a][1,3,5]triazine Ring System Leading to a Range of Substituents in the 2, 5 and 7 Positions. *J. Chem. Soc. [Perkin 1]* **1995**, No. 7, 801.

(30) Caulkett, P. W. R.; Jones, G.; Collis, M. G.; Poucher, S. M. Azole Derivatives. EP0459702A1.

(31) Floris, M.; Sabbadin, D.; Medda, R.; Bulfone, A.; Moro, S. Adenosiland: Walking through Adenosine Receptors Landscape. *Eur. J. Med. Chem.* **2012**, *58*, 248–257.

(32) Klotz, K. N.; Hessling, J.; Hegler, J.; Owman, C.; Kull, B.; Fredholm, B. B.; Lohse, M. J. Comparative Pharmacology of Human Adenosine Receptor Subtypes - Characterization of Stably Transfected Receptors in CHO Cells. *Naunyn. Schmiedebergs Arch. Pharmacol.* **1998**, *357* (1), 1–9.

(33) De Lean, A.; Hancock, A. A.; Lefkowitz, R. J. Validation and Statistical Analysis of a Computer Modeling Method for Quantitative Analysis of Radioligand Binding Data for Mixtures of Pharmacological Receptor Subtypes. *Mol. Pharmacol.* **1982**, *21* (1), 5–16.

(34) Klotz, K. N.; Cristalli, G.; Grifantini, M.; Vittori, S.; Lohse, M. J. Photoaffinity Labeling of A1-Adenosine Receptors. *J. Biol. Chem.* **1985**, *260* (27), 14659–14664.

(35) Yung-Chi, C.; Prusoff, W. H. Relationship between the Inhibition Constant (KI) and the Concentration of Inhibitor Which Causes 50 per Cent Inhibition (I50) of an Enzymatic Reaction. *Biochem. Pharmacol.* **1973**, *22* (23), 3099–3108.

(36) Molecular Operating Environment (MOE), 2014.09; Chemical Computing Group Inc., 1010 Sherbooke St. West, Suite #910, Montreal, QC, Canada, H3A 2R7, 2015.

(37) *GOLD Suite, Version 5.2*; Cambridge Crystallographic Data Centre: 12 Union Road, Cambridge CB2 1EZ, UK.

(38) Liu, W.; Chun, E.; Thompson, A. A.; Chubukov, P.; Xu, F.; Katritch, V.; Han, G. W.; Roth, C. B.; Heitman, L. H.; IJzerman, A. P.; Cherezov, V.; Stevens, R. C. Structural Basis for Allosteric Regulation of GPCRs by Sodium Ions. *Science* **2012**, *337* (6091), 232–236.

(39) Floris, M.; Sabbadin, D.; Medda, R.; Bulfone, A.; Moro, S. Adenosiland: Walking through Adenosine Receptors Landscape. *Eur. J. Med. Chem.* **2012**, *58*, 248–257.

(40) Floris, M.; Sabbadin, D.; Ciancetta, A.; Medda, R.; Cuzzolin, A.; Moro, S. Implementing the "Best Template Searching" Tool into Adenosiland Platform. *Silico Pharmacol.* **2013**, *1* (1), 25.

(41) Ballesteros, J. A.; Weinstein, H. [19] Integrated Methods for the Construction of Three-Dimensional Models and Computational Probing of Structure-Function Relations in G Protein-Coupled Receptors. In *Methods in Neurosciences*; Elsevier, 1995; Vol. 25, pp 366–428.

(42) Labute, P. Protonate3D: Assignment of Ionization States and Hydrogen Coordinates to Macromolecular Structures. *Proteins* **2009**, *75* (1), 187–205.

(43) Ciancetta, A.; Cuzzolin, A.; Moro, S. Alternative Quality Assessment Strategy to Compare Performances of GPCR-Ligand Docking Protocols: The Human Adenosine A $_{2A}$ Receptor as a Case Study. *J. Chem. Inf. Model.* **2014**, *54* (8), 2243–2254.

- A series of triazolo-triazines was developed as adenosine receptor (AR) antagonists
- Compounds show better affinity at the hA_{2A} and hA_3 ARs than at the hA_1 and hA_{2B} ARs
- A benzylamino group at the C5 position gives highest affinity values at the hARs
- Docking simulations were carried out to explain the observed binding data